

NAVAL POSTGRADUATE SCHOOL

Monterey, California



THESIS

**EVALUATION OF THE THERMAL CONTROL
SYSTEM OF THE PETITE AMATEUR NAVY
SATELLITE (PANSAT)**

by

Nicholas M. Davinic

June, 1995

Thesis Advisor: Prof. Allan Kraus

Approved for public release; distribution is unlimited.

19960221 049

DTIC QUALITY INSPECTED 1

Unclassified

SECURITY CLASSIFICATION OF THIS PAGE

Form Approved
OMB No. 0704-0188**REPORT DOCUMENTATION PAGE**

1a. REPORT SECURITY CLASSIFICATION Unclassified			1b. RESTRICTIVE MARKINGS		
2a. SECURITY CLASSIFICATION AUTHORITY			3. DISTRIBUTION/AVAILABILITY OF REPORT Approved for public release; distribution is unlimited		
2b. DECLASSIFICATION/DOWNGRADING SCHEDULE					
4. PERFORMING ORGANIZATION REPORT NUMBER(S)			5. MONITORING ORGANIZATION REPORT NUMBER(S)		
6a. NAME OF PERFORMING ORGANIZATION Naval Postgraduate School		6b. OFFICE SYMBOL (If applicable)		7a. NAME OF MONITORING ORGANIZATION Naval Postgraduate School	
6c. ADDRESS (City, State, and ZIP Code) Monterey, CA 93943-5000		7b. ADDRESS (City, State, and ZIP Code) Monterey, CA 93943-5000			
8a. NAME OF FUNDING/SPONSORING ORGANIZATION		8b. OFFICE SYMBOL (If applicable)		9. PROCUREMENT INSTRUMENT IDENTIFICATION NUMBER	
8c. ADDRESS (City, State, and ZIP Code)			10. SOURCE OF FUNDING NUMBERS		
			PROGRAM ELEMENT NO.	PROJECT NO.	TASK NO.
			WORK UNIT ACCESSION NO.		
11. TITLE (Include Security Classification) EVALUATION OF THE THERMAL CONTROL SYSTEM OF THE PETITE AMATEUR NAVY SATELLITE (PANSAT)					
12. PERSONAL AUTHOR(S) Nicholas M. Davinic					
13a. TYPE OF REPORT Master's Thesis		13b. TIME COVERED FROM _____ TO _____		14. DATE OF REPORT (Year,Month,Day) June 1995	
				15. PAGE COUNT 88	
16. SUPPLEMENTARY NOTATION The views expressed in this thesis are those of the author and do not reflect the official policy or position of the Department of Defense or the U.S. Government.					
17. COSATI CODES			18. SUBJECT TERMS (Continue on reverse if necessary and identify by block number)		
FIELD	GROUP	SUB-GROUP			
			Thermal Analysis, Spacecraft, PANSAT, ITAS		
19. ABSTRACT (Continue on reverse if necessary and identify by block number) A thermal management system is required on satellites to maintain spacecraft components within prescribed temperature limits. This thesis describes the development of an analytical thermal model for the PANSAT satellite. The analytical model is used to characterize the thermal environment and temperature fluctuations on board the PANSAT spacecraft while operational in the space environment. The model is developed and interrogated in the Integrated Thermal Analysis System (ITAS) environment. In addition to documenting the model, and the assumptions and methodology used in developing the model, the thesis will attempt to define an appropriate test philosophy for subsequent environmental testing of the PANSAT spacecraft. The thesis text will serve as the primary documentation for the thermal model so that it can be fully utilized to support required environmental testing.					
20. DISTRIBUTION/AVAILABILITY OF ABSTRACT <input checked="" type="checkbox"/> UNCLASSIFIED/UNLIMITED <input type="checkbox"/> SAME AS RPT. <input type="checkbox"/> DTIC USERS			21. ABSTRACT SECURITY CLASSIFICATION Unclassified		
22a. NAME OF RESPONSIBLE INDIVIDUAL Allan Kraus			22b. TELEPHONE (Include Area Code) (408) 656 - 2730		22c. OFFICE SYMBOL EC/Ts

DD Form 1473, JUN 86

Previous editions are obsolete.

S/N 0102-LF-014-6603

SECURITY CLASSIFICATION OF THIS PAGE

Unclassified

Approved for public release; distribution is unlimited.

**EVALUATION OF THE THERMAL CONTROL SYSTEM OF THE PETITE
AMATEUR NAVY SATELLITE (PANSAT)**

**Nicholas M. Davinic
Naval Research Laboratory
B.S.M.E., George Washington University, 1987**

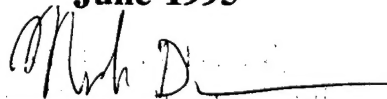
Submitted in partial fulfillment of the requirements for
the degree of

**MASTER OF SCIENCE IN ASTRONAUTICAL
ENGINEERING**

from the

**NAVAL POSTGRADUATE SCHOOL
June 1995**

Author:



Nicholas M. Davinic

Approved by:



Allan Kraus, Thesis Advisor



Nelson Hyman, Second Reader



**Daniel Collins,, Chairman, Department of Aeronautics and
Astronautics**

ABSTRACT

A thermal management system is required on satellites to maintain spacecraft components within prescribed temperature limits. The focus of this thesis is the development of an analytical thermal model for the PANSAT satellite. The thermal model will be used to characterize the thermal environment and temperature fluctuations on board the PANSAT spacecraft while in operation. The model is developed and interrogated in the Integrated Thermal Analysis System (ITAS) environment. In addition to documenting the model, and the assumptions and methodology used in developing the model, the thesis will attempt to define an appropriate test philosophy for subsequent environmental testing of the PANSAT spacecraft. The thesis text will serve as the primary documentation for the thermal model so that it can be fully utilized to support required environmental testing.

TABLE OF CONTENTS

I. INTRODUCTION.....	1
A. PANSAT BACKGROUND.....	1
B. SPACECRAFT THERMAL CONTROL.....	1
C. THERMAL CONTROL SYSTEM DESIGN.....	2
II. THERMAL MODEL DEVELOPMENT.....	7
A. INTEGRATED THERMAL ANALYSIS SYSTEM	
(ITAS) BACKGROUND.....	7
B. PANSAT MODEL.....	8
1. Geometry.....	8
2. Payload Electronics.....	9
3. Thermal Nodes.....	10
4. Black Body View Factors, Radiation	
Interchange Factors, and Shadow Factors.....	14
5. Orbital Parameters.....	17
6. Attitude.....	17
7. Linear Conductances	18
III. MODEL EVALUATION.....	25
A. ANALYTICAL THERMAL MODEL SOLUTION....	25
B. RESULTS.....	27
1. Hot Case.....	28
2. Cold Case.....	33
3. Sensitivity Studies.....	36
IV. PANSAT THERMAL TESTING.....	43
A. THERMAL TESTING IN THE DESIGN PROCESS.....	43
B. SYSTEM LEVEL THERMAL TESTING.....	43
1. Thermal Design Verification Test.....	43
2. Thermal Vacuum Testing.....	46
3. PANSAT Testing.....	46

V. CONCLUSIONS.....	4 9
APPENDIX A.....	5 1
APPENDIX B.....	6 1
APPENDIX C.....	6 3
APPENDIX D.....	7 1
REFERENCES.....	7 7
INITIAL DISTRIBUTION LIST.....	7 9

I. INTRODUCTION

A. PANSAT BACKGROUND

The PANSAT satellite is being developed at the Naval Postgraduate School (NPS) to demonstrate the feasibility of a quick reaction, low cost communications satellite. The satellite will provide digital over the horizon communications and uses direct sequence spread spectrum UHF packet communications. The payload will be used to evaluate the performance of spread spectrum communications using the amateur radio operator community as the user base. PANSAT will also serve as a valuable educational tool for NPS students by providing them an opportunity to work on real satellite hardware. Students at NPS are responsible for the design and development of the PANSAT system. The work done for this particular thesis will satisfy the critical requirement of developing an analytical thermal model to support spacecraft design, integration, and test.

B. SPACECRAFT THERMAL CONTROL

The function of the thermal control subsystem (TCS) on any spacecraft is to maintain selected onboard components within specified temperature limits during all phases of the mission. Of primary concern is the operational on-orbit phase of the mission. The TCS design must account for all environmental (**Figure 1**) and internal thermal inputs including direct and reflected solar, and earth radiative fluxes, and heat dissipation from spacecraft electronics. The satellite maintains an energy balance between the various external and internal heat loads. The satellite TCS helps to maintain that balance in a way that ensures that all critical components are maintained within required temperature limits [Reference 1].

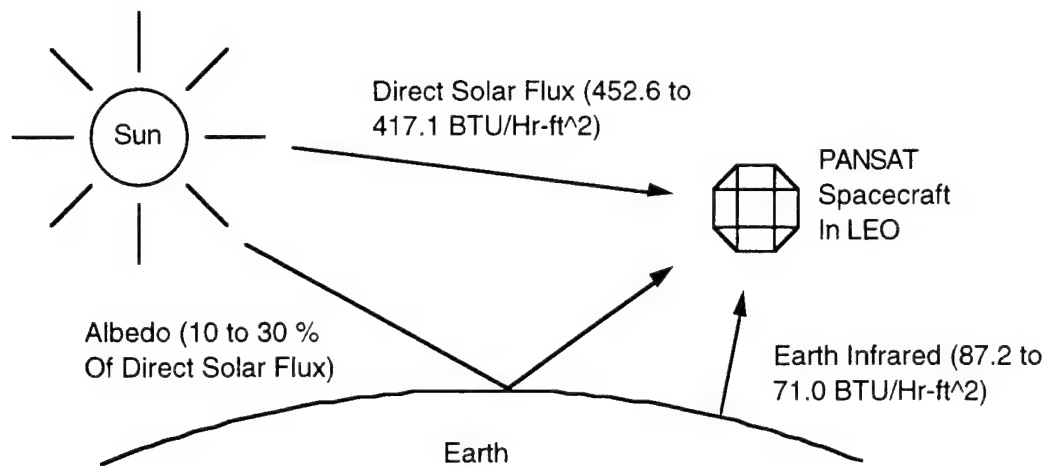


Figure 1. Satellite Thermal Environment

In addition to ensuring survival of components while on-orbit, the spacecraft TCS must ensure that components are not adversely affected in any of the less stressing environments seen by the system. These environments include launch processing and pre-launch conditions in the fairing, ascent in the fairing, and pre-operational on-orbit modes such as acquisition. This thesis will only address thermal performance during the on-orbit phase of the PANSAT mission. It is believed that all other phases are enveloped by the on-orbit conditions.

C. THERMAL CONTROL SYSTEM DESIGN

The TCS design process involves significant interaction with the other spacecraft subsystems, such as the electrical power subsystem and the structural subsystem. Temperature limits for various components are defined by the individual subsystems. Evaluation of possible spacecraft geometries and thermal management equipment is conducted in the early phases of the design process by using simple analytical models to define spacecraft heat balances. Most of the early design work is done using steady state assumptions and usually two conditions; the worst case hot case and the worst case cold

case are used for evaluation of design options. As the design matures, more detailed analytical models are developed to define the thermal characteristics of the spacecraft. A number of software products have been developed for this very specific problem, including SINDA (developed by NASA) and ITAS (developed by the Analytix Corp.). These models discretize the spacecraft into a finite number of isothermal entities commonly referred to as thermal nodes. By correctly defining the thermal connectivity (i.e. conduction, radiation, or convection coupling) between these nodes, and assigning appropriate thermal characteristics (i.e. thermal mass, surface optical properties), the spacecraft can be subjected to various heat loads and environments. The energy flow can be traced throughout the various satellite elements, and component temperatures predicted. These models can be used for steady state analyses and more importantly transient analyses can be performed to predict real time thermal performance of the spacecraft system and individual components. A typical spacecraft thermal design process is presented in **Figure 2**, [Reference 2].

This thesis develops the first detailed analytical thermal model for the PANSAT project. Most of the preliminary system level trade studies regarding configuration, sizing, and other areas have been completed without a detailed model. This thermal model will be used to validate the current PANSAT design and also support subsequent testing. This model is not intended to be a final step in the design process; instead it should be used to optimize the PANSAT design as well as be verified itself through later correlation with test data.

Sometime after the overall thermal design is finalized, the spacecraft, or in some cases a qualification unit, is subjected to a thermal design verification test. In this test the space environment is usually simulated by placing the vehicle in a thermal vacuum chamber and

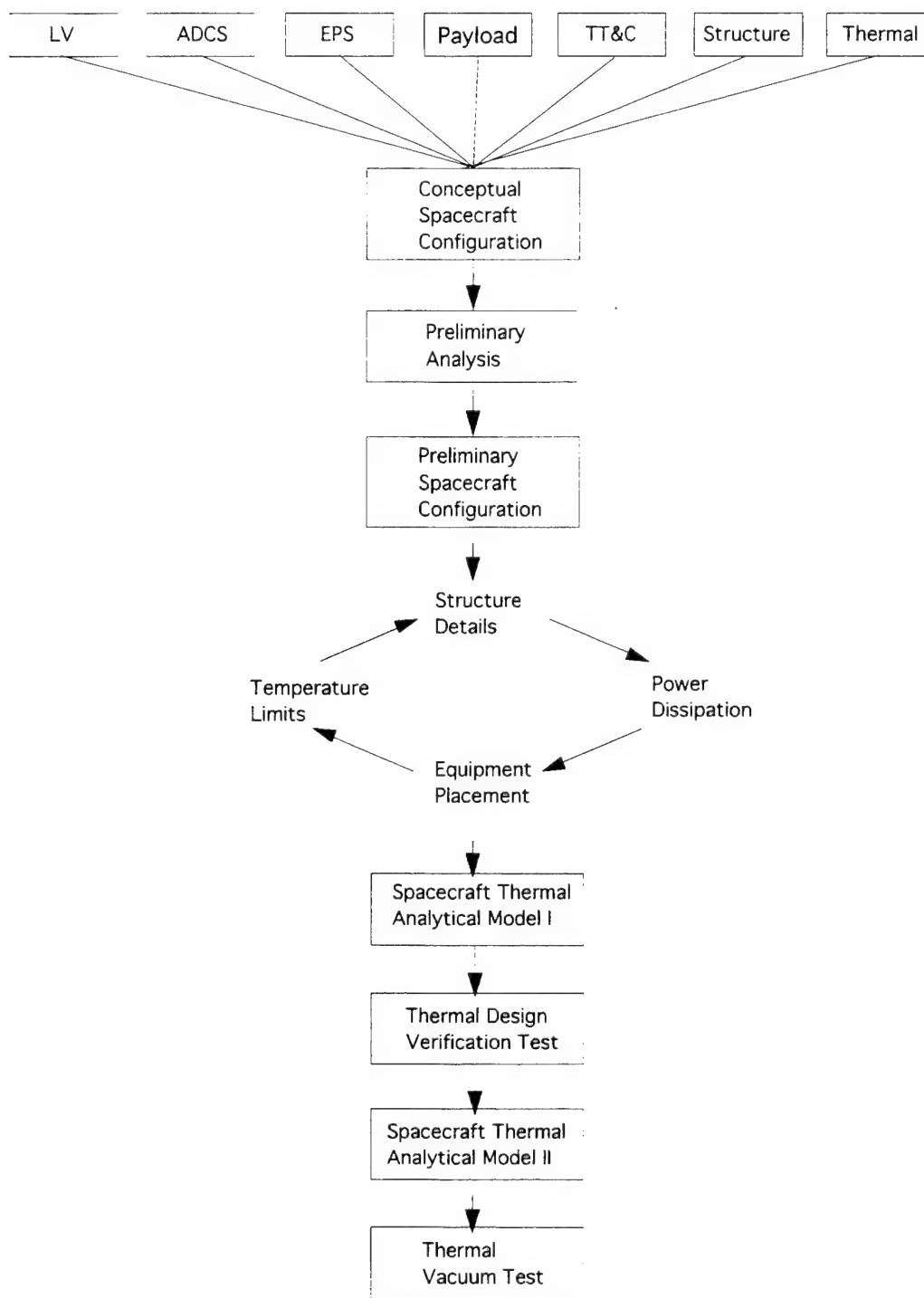


Figure 2. Satellite Thermal Design Approach

subjecting it to the known environmental extremes, usually a cold case in eclipse with the minimum internal loads and a hot case with the highest internal loads and the spacecraft in full sun. This test is not intended to qualify any components but is primarily used to verify the thermal control system and validate the analytical thermal model. External heat loads may be simulated using lamps or surface mounted strip heaters and a cold shroud can be used to simulate the space sink. Spacecraft equipment heat dissipations are simulated by resistive heaters or, when available, electrical simulators (component qualification units). After all the data is collected, reduced, and evaluated it can be used to validate the selected thermal design and the analytical thermal model. More detailed information on how this model is used to support thermal testing is included in Chapter IV.

Later in the development program, the flight vehicle is subjected to a thermal vacuum test which involves subjecting the system to a program defined set of worst case hot/cold cycles. Analytically predicted temperature extremes are used to help define the test conditions, but the objective of this test is flight systems acceptance and there is no other relation to the TCS. A single flight unit, however, may be used for both the early thermal design verification test and the later thermal vacuum test, without the benefit of a separate qualification unit. Again, the analytical model is used as a predictive tool in the design process and is verified, or modified if necessary, based on correlation with test data.

PANSAT is expected to undergo thermal design verification and thermal vacuum testing prior to acceptance for flight. It is expected that the analytical model developed for this thesis will be used as the baseline thermal model which will be updated and validated by subsequent testing. Adequate documentation is provided in this thesis, and in any supplemental text if required, to allow for modification of the analytical model based on results from thermal testing.

1

II. THERMAL MODEL DEVELOPMENT

A. INTEGRATED THERMAL ANALYSIS SYSTEM (ITAS) BACKGROUND

The analytical thermal model developed to describe the PANSAT spacecraft has been created using the ITAS. ITAS is a fully integrated thermal analysis package, specially developed for use in satellite thermal design. The package is menu driven, user friendly, and runs on all 80386PC (or better) platforms. Facilities at both NRL and NPS are available to support future ITAS models or modifications of this model as PANSAT thermal test data becomes available.

ITAS supports all relevant functions of system level analytical thermal design. Spacecraft geometry is generated internal to ITAS using the geometry building task and its library of geometric entities such as plates, boxes, and spheres. Entire satellites or individual components can be modeled with as much detail as necessary. View factors can be generated for systems using either contour integration or Monte Carlo ray tracing algorithms. Shadow factors or blockage factors can be generated. Radiation interchange factors can be generated for either diffuse or specular reflective surfaces. On-orbit incident flux calculations as well as absorbed heat rate calculations can be used later for steady state or transient temperature solutions. The thermal solutions used by ITAS are functionally equivalent to NASA/SINDA's STDSTL and FWDBCK solutions. ITAS can serve as a pre processor by generating data decks compatible with the SINDA and TRASYS codes used in many facilities. ITAS can aid in interrogating analysis results, either from internal ITAS solutions or imported results from SINDA by applying ITAS graphical capabilities such as time history plots of component temperatures.

B. PANSAT MODEL

1. Geometry

The first step in developing an analytical thermal model of the PANSAT spacecraft is to discretize the system into a manageable number of thermal nodes. These nodes would then be assembled with the appropriate connectivity and submitted to the ITAS finite difference analysis engine for both steady state and transient analyses. Geometry related thermal nodes used in the PANSAT model are developed using the internal geometry generation task. These nodes represent the various structural elements as well as the payload electronics components.

The overall PANSAT model geometry is given in **Figure 3**. Detailed drawings of the spacecraft structural elements are provided in Appendix A. The PANSAT structure can be described as a faceted 19 in. diameter sphere. The structure is assembled from 29 individual structural members. The spherical shell uses 26 individual plates, some of which are flat 0.063 in. thick aluminum sheets others are machined 0.25 in. thick aluminum plate. Over 80% of the material is removed on the machined parts leaving an isogrid geometry with a 0.063 in thick plate with 0.25 in. high ribs. There are twelve machined rectangular plate elements used in the outer shell construction. Eight triangular and six rectangular aluminum sheet panels are used to closeout the sphere. The internal volume of the PANSAT satellite is divided into three separate volumes by two internal decks. The three volumes have no view to space nor to each other. The two decks are used to mount the payload electronics. The upper deck is a solid 0.25" thick aluminum plate. The lower deck is a 0.25 in thick aluminum plate that has been machined down to 0.125 in. thickness over most of its surface area (edges are still 0.25 in.). The lower deck attaches directly to an internal thrust tube which is the primary attachment point to the launch system separation hardware. The thrust tube is a single piece aluminum construction.

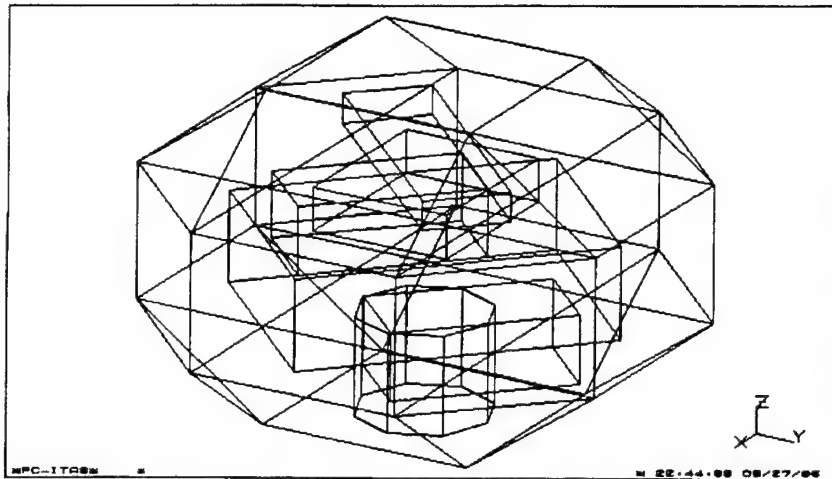


Figure 3. PANSAT Thermal Model (Outer Geometry And Sub Enclosures)

All the geometric surfaces were created using the ITAS geometry definition module and stored in a separate parts file. This parts file is used later in developing the individual thermal nodes and sub-models. All user generated files are given listed in Appendix B.

2. Payload Electronics

The payload electronics consist of five individual boxes. The Radio Frequency Communications Module (RFCM) is located on the +Z surface of the upper equipment panel. The Electrical Power Module (EPM) is located on the -Z surface of the upper equipment panel. The Digital Control Module (DCM) and both Battery A and Battery B are located on the +Z surface of the lower equipment panel. There are no electronics located in the lowest bay. Pertinent box information is given in Table 1. The source of this information is the PANSAT PDR package. It is assumed that a space qualified mounting interface gap filler, such a room temperature vulcanized (RTV) silicon rubber compound is used in mounting the boxes to the decks to increase thermal conductance coupling. Stainless steel 4-40 fasteners are used for assembly of the structure and are assumed to be used for mounting the electronics boxes.

Component	Length (in)	Width (in)	Height (in)	Mass (lbs)	Power Peak (W)	Number Of Fasteners
RFCM	10	3	1.5	12	8	6
EPM	6	5.5	2.25	8	5 (est.)	8
DCM	11	8.25	4.75	10	3	8
Battery A	6.39	3.37	3.5	8	5 (est)	6
Battery B	6.39	3.37	3.5	8	5 (est)	6

Table 1. Component Summary

3. Thermal Nodes

The ITAS geometry generation task is used to develop a surface geometry that described all the significant components for thermal analysis. These surfaces are selected as thermal nodes for the PANSAT model. This is done by developing an assembly of surfaces from the existing parts file (actually a subset of all available surface in parts file) and loading the surfaces into ITAS. ITAS automatically assigns node numbers to individual surfaces (these number can be changed by the user to aid in book keeping later). It is important to distinguish between surfaces, which are simply geometric entities, and thermal nodes which are single point, lumped parameter representations of physical hardware. Thermal nodes carry all pertinent thermal information (geometry, surface optical properties, thermal mass, thermal dissipations) that will characterize a component and be used in analysis.

Some simplifications were made in developing these thermal nodes, such as ignoring the internal ribs on the rectangular shell structural panels. Instead the panels were modeled as flat plates with the equivalent weight of the actual ribbed parts. External view factors for the environmental inputs are not effected by this simplifying assumption because the ribs are on the inside of the vehicle. The radiation coupling between components on the inside

of the vehicle may be slightly off because the ribs may cause some internal shadowing. The ribs are only 0.25 in high and all the electrical components have views that are nearly normal to the panel surfaces, thus shadowing should be insignificant. In addition, it was assumed that these panels were isothermal due to their small size and the high thermal conductivity of aluminum. This assumption was not made for the equipment panels and they were modeled as a collection of discrete nodes that were later linked with appropriate conductance values.

After the individual components were constructed and saved in a separate parts file the configuration of the vehicle used for analysis was selected. In complicated spacecraft with deployable and movable elements the selection of appropriate configurations for analysis can impact the results significantly. The PANSAT satellite does not have any moving parts and the geometry is fixed through time.

The configuration of the vehicle was such that the internal volume was actually divided into three sub-enclosures that did not have any field of view to space, nor to each other. This fact allowed for modeling the sub-enclosures as separate cavities. In this way the satellite model was divided into four sub-models: an exterior model that consisted of the outward facing surfaces of the faceted shell geometry and the three separate internal sub-enclosures. The four sub models are shown in Figures 4 - 7. This practice of using sub-enclosures allows for much lower computation times for the final thermal analyses because the matrices that define the view factors and radiation conductances between all entities are partitioned and smaller. Analytically decoupling cavities that are decoupled in terms of radiation interchange serves to simplify analyses without sacrificing accuracy.

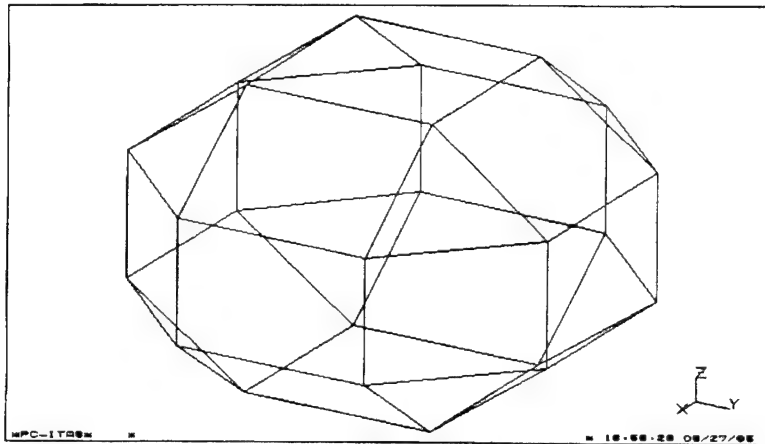


Figure 4. Outer Surfaces Model

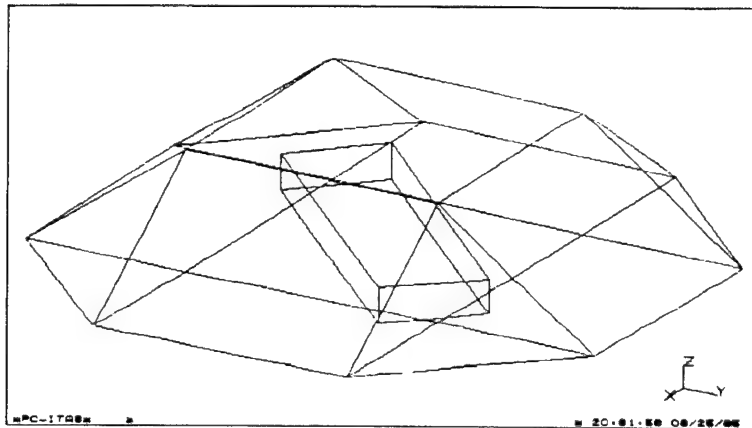


Figure 5. Upper Bay Enclosure

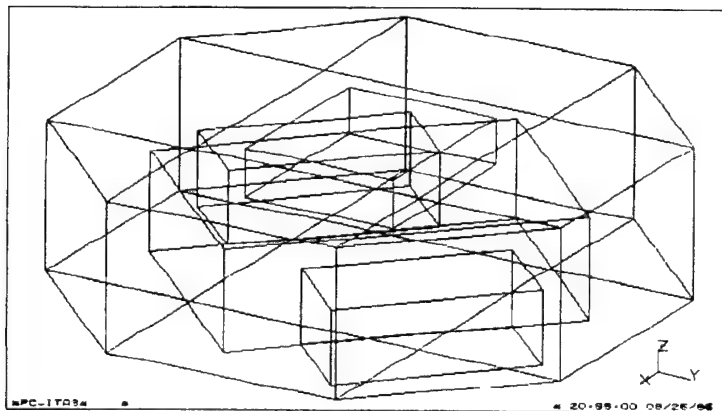


Figure 6. Middle Bay Enclosure

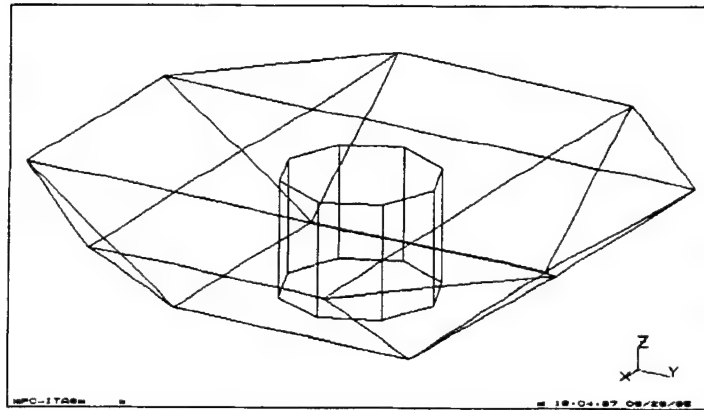


Figure 7. Lower Bay Enclosure

After the geometry is generated certain parameters associated with the geometry need to be defined. The first step is to clearly identify which surfaces will become thermal nodes recognized as such in the ITAS environment. A surface is a purely geometric entity. The relationship between a surface and a thermal node needs to be defined explicitly. Once this is done additional properties, such as thermal mass and heat dissipation, are assigned to the thermal nodes as well. A one to one correspondence need not be maintained between thermal nodes and surfaces. A single node may be comprised of several surfaces (a single surface cannot be referenced to two thermal nodes). This construct implies that the surfaces are isothermal with respect to each other and any additional properties such as thermal mass are shared. This approach is employed in the modeling the of electronics boxes. The top and side surfaces of a box are made part of a single thermal node thus reducing later work in defining conductances between side walls and making the box behave as an isothermal entity. This single thermal node is linked to a node representing the base of the box via a linear conductance (see section 6). If more accurate box analysis is required the box can be modeled in more detail, even to the point of making it a separate enclosure within the spacecraft system level thermal model.

Surface optical properties of all components play a key role in the thermal analysis. Each thermal node was assigned an absorptivity (α), and an emissivity (ϵ) in accordance with the selected surface coatings. These values were not completely defined at the time work on this model began and it is assumed that surface optical properties of all internal components can be modified as required to provide appropriate radiative conductances. The use of anodizes or other chemical conversion processes or thermal paints, is considered a feasible engineering option. For an initial condition it was assumed that the surfaces are solvent cleaned aluminum 7075-T6.

The thermal mass or capacitance of a node defines its transient behavior. Capacitance is the product of the mass associated with the node and the specific heat of the material comprising that mass (0.2 Btu/lb-°F for aluminum). Each structural node is assigned a thermal mass, but the mass of an electronics box was assigned slightly differently. Each box consisted of two nodes, one for the base, and one for the remaining five sides. All of the thermal mass was attributed to the node representing the side walls and then the base node was linked to the side wall node with a linear conductance. This would allow for further fine tuning of the model once test data becomes available by modifying conductance values and thermal masses. Appendix C lists all the thermal nodes used in the PANSAT model and pertinent parameters.

4. Black Body View Factors, Radiation Interchange Factors, And Shadow Factors

The use of individual sub-enclosures in the PANSAT model reduces computing time considerably. Each of these sub-enclosure models is used to develop the radiation interchange factors, commonly referred to as Script-Fs, associated with each cavity. It is important to realize that each cavity is a stand alone thermal model used only to generate radiation interchange factors between the entities internal to the cavity. These radiation interchange factors are stored in a separate file (RADK file) which is used in the all

inclusive thermal model later. Appropriate linear conductions are used to define the connectivity of the sub enclosure entities to the external model.

Before radiation interchange factors can be calculated, black body view factors must be determined. View factors define the energy exchange between two black surfaces. This relationship is given by [Reference 3],

$$E_{b1}A_1F_{12} - E_{b2}A_2F_{21} = Q_{1-2} \quad (1)$$

Where,

F_{12} = Fraction of energy leaving surface 1 which reaches surface 2

F_{21} = Fraction of energy leaving surface 2 which reaches surface 1

A_n = Surface area

E_{bn} = Total energy emitted by body

Q_{1-2} = Net heat exchange

View factors are calculated using contour integration techniques. Parameters defining number of surface sub-divisions (i.e. mesh size) used in the calculation are defined by the user. To determine the appropriate number of surfaces, enclosure view factors are computed and the summations from each of the surfaces are compared to unity. Increasing the mesh density results in this summation more closely approaching one.

The Script-Fs are used in the complete thermal analysis to account for all thermal radiation interchange. Script-Fs are calculated from the Black-Body radiation view factors in conjunction with relevant surface optical properties by a series of matrix operations. The Script-Fs used for the PANSAT model were defined using the following formula (Gebhart formula, Reference 4):

$$SF = E \cdot [(I - BBVF \cdot E)^{BBVF} - 1] \cdot BBVF \cdot E \quad (2)$$

Where,

SF = Script-F Matrix

E = Emmitance Matrix

I = Unit Matrix

$BBVF$ = Black-Body View Factor Matrix

The summation of all Script-Fs from a surface to all other surfaces in an enclosure should be equal to the emissivity of that surface. Generation of the radiation interchange factors by Equation (2) is acceptable if the surfaces are diffuse. All surfaces in the PANSAT model are assumed diffuse. If the surfaces are specular reflectors then a Monte Carlo Ray tracing algorithm can be used. The Gebhart method is a two step process where the BBVFs are first calculated and are then used in conjunction with the surface optical properties. Monte Carlo Ray tracing is a single step process that calculates the final interchange factors directly using all the actual values of the emmissivities. Computer time is increased by an order of magnitude if ray tracing is selected and should be avoided as much as possible [Reference 5].

ITAS also accounts for any blockage or shadowing that occurs during incident flux calculations. Due to the convex spherical geometry there are no structural surface that would create any shadows. The whip antennas create negligible shadowing and are not included in the model because they have no appreciable impact on the thermal characteristics of the PANSAT satellite. Parameters defining the accuracy of this calculation are also user modifiable, but no attempt was made to change the recommended default parameters.

5. Orbital Parameters

In ITAS detailed information regarding environmental parameters and on station spacecraft attitude is provided via the orbital analysis input forms. The principal on orbit environmental heat loads are direct incident radiation from the sun, reflected sun from the surface of the earth (albedo), and earth infrared energy. Most of the solar and albedo radiation is in the ultraviolet part of the spectrum, while the earth radiation is in the infrared. Environmental inputs are defined using solar vector definition angles, typically referred to as beta angles, or through explicit orbit definition. Definition using orbital elements was selected primarily for familiarity and ease of use. The orbital elements are given in Table 2. The information was taken from the Space Test Program (STP) flight request executive summary submitted to STP in January 1993.

Inclination	28.5
Longitude of Ascending Node	Not specified for PANSAT
Perigee	480 + 200 km
Apogee	Circular Orbit

Table 2. Orbital Parameters

6. Attitude

Although attitude has a direct impact on the thermal performance of most spacecraft, the uniform external PANSAT geometry and optical properties result in a net energy balance that is unaffected by the spacecraft attitude, however, internal thermal gradients can be influenced by vehicle orientation. While PANSAT does not have any attitude control hardware, there are two most likely preferred on-station attitudes. First, although the external geometry is spherical, the moments of inertia are not all equal so a gravity gradient torque may develop that serves to position the vehicle in a permanently earth facing orientation. A second possible attitude would be an uncontrolled tumble that is affected by constantly changing interaction of external torques such as solar pressure torques, gravity

gradient torques, and aerodynamic drag. In the earth facing attitude there would be a greater chance for internal thermal gradients to arise because surfaces would be exposed to certain sources for prolonged periods of time. In the tumble mode the tendency would be towards reducing internal gradients as long as tumble rates were appreciable. Both the earth facing and tumble attitudes need to be examined. With unknown inertia ratios any side of the vehicle may become the earth facing side. The same holds for the tumble mode, in which more than one orientation of the spin axis is possible.

7. Linear Conductances

In addition to radiative conductances between nodal elements, linear conductances are defined where appropriate. Linear conductances define the conductive heat flow between components as shown in equation (3). Linear conductances become part of the overall model and are not part of any of the sub enclosure models.

$$Q = -kA\left(\frac{dT}{dx}\right) \quad (3)$$

Where,

Q = Heat transfer rate

k = Thermal conductivity

A = Cross sectional area

$\left(\frac{dT}{dx}\right)$ = Temperature gradient in the direction of heat flow

There are three different types of linear conductance that are used in the PANSAT thermal model. The first is used to couple adjacent nodes that are actually part of the same contiguous structural member. In this case the conductance between adjacent nodes is defined as,

$$C = \frac{kA}{L} \quad (4)$$

Where,

C = Linear conductance

k = Thermal conductivity

A = Cross sectional area between nodes

L = Distance between nodes (node locations taken to be centroid of surface)

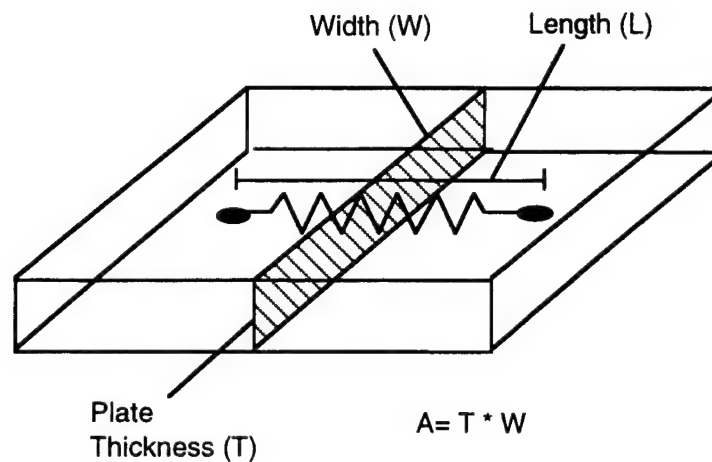


Figure 8. Geometry Used For Linear Conductance

This type of conductance is used to couple nodes on the equipment decks. The decks were discretized because they are relatively large and will have localized thermal inputs from attached boxes. Both of these conditions suggest that the decks will not be isothermal and will develop thermal gradients. Each deck is modeled with a total of eighteen nodes, nine nodes for the top surface and nine nodes for the bottom. The connectivities are shown in **Figure 9**. Due to symmetry the same values for conductance appear in several locations. Each equipment deck required eight C1 conductances, sixteen C2 conductances, and nine C3 conductances. Conductance values are given in Table 3. Because each equipment deck is common to two sub enclosures, i.e. the top surface of the upper equipment deck is part

of the top enclosure, while the lower surface of the same deck is part of the middle enclosure, the cross sectional area used in conductance calculations is divided evenly

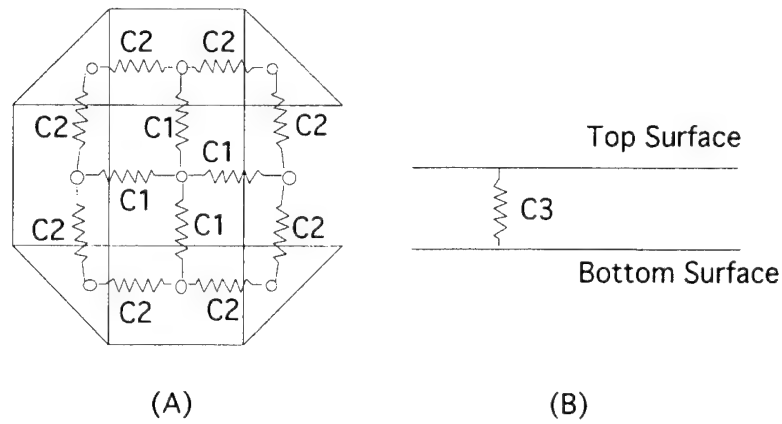


Figure 9. Equipment Deck Conduction Network

	Conductivity (BTU/ Hr-ft-F)	Thickness (in)	Width (in)	A (in)	L (in)	Cn (BTU/ Hr-F)
Top Deck						
C1	94.0	0.25	7.625	0.95	6.2	1.2
C2	94.0	0.25	4.80	0.60	5.9	0.8
Bot. Deck						
C1	94.0	0.125	7.625	0.48	6.2	0.6
C2	94.0	0.125	4.80	0.30	5.9	0.4
Top Deck						
C3 (side sq)	94.0	7.62	4.8	36.6	0.25	1146
C3 (cen sq)	94.0	7.62	7.62	58.1	0.25	1820
C3 (tri)	94.0	4.8	4.8	11.5	0.25	360
Bot. Deck						
C3 (side sq)	94.0	7.62	4.8	36.6	0.125	1146
C3 (cen sq)	94.0	7.62	7.62	58.1	0.125	1820
C3 (tri)	94.0	4.8	4.8	11.5	0.125	360

Table 3. Deck Conductances

between the upper and lower surface of each deck. The C3 conductance is used to tie sub-enclosures together and allow heat transfer through the thickness of an equipment deck.

Linear conductances for structural joints must account for contact conductances between mating parts. Two apparently smooth surfaces under uniform pressure are subject to a complex heat exchange phenomenon due to microscopic roughness. As depicted in **Figure 10** the actual contact surfaces between two structural members are not perfectly smooth.

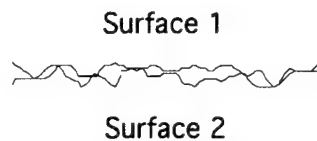


Figure 10. Microscopic Interface Surface Roughness

Radiative, conductive, and convective heat transfer are typically all present across this type of interface. In the vacuum environment of space no convective heat transfer is possible. At moderate temperatures (-60 to 180 deg F) the radiative component is insignificant. Conduction is therefore the dominant mode of heat transport. A number of analytical solutions for the uniform pressure problem have been proposed [Reference 6]. Unfortunately real world mechanically fastened joints do not have a uniform pressure distribution, but instead the pressure distribution is a function of the fastener design, proximity to the fastener, and overall joint geometry (thickness, free edge effects). A limited amount of empirical data exists for mechanically fastened joints in vacuum, specifically aluminum plates bolted together with stainless steel fasteners [Reference 7]. The PANSAT structure uses threaded mechanical fasteners, UNC 4-40 stainless, throughout the assembly. A summary table for bolted joint conductances is given as Table 4. The values for the 4-40 fasteners is extrapolated from existing data on larger fasteners. These conductance values are for a single bolt joint. The net conductance values for each joint depend on the number of fasteners and the net thickness. For example, for PANSAT

joints mating two machined components, such as at the equipment deck to machined solar array panel, 0.5 in thickness was assumed. For PANSAT joints attaching a machined component to a sheet metal component, such as the joint between a machined solar array panel and a sheet metal panel, a 0.125 in thickness was assumed.

Bolt Size	Finish Microinch	Mean Thickness inch	Conductance BTU/hr-F	Source
8-32	50	0.125	0.79	Reference 5
8-32	25	0.5	3.14	Reference 5
6-32	50	0.125	0.55	Reference 5
6-32	25	0.5	2.20	Reference 5
4-40	50	0.125	0.31	Extrapolated
4-40	25	0.5	1.26	Extrapolated

Table 4. Structural Joint Conductance Values

Another unique set of linear conductances used in the PANSAT model accounts for heat transfer between electronics boxes and the surfaces to which they are mounted. This is also an area that has some analytical solutions, but conductances based on empirical data are regarded as more accurate. **Figure 11** is a graph developed and used in industry for determining overall contact conductances for electronics boxes mounted using perimeter bolt patterns [Reference 8]. Values for both bare interfaces and RTV interfaces are provided. The use of RTV is a commonly accepted practice when boxes are installed on surfaces that are used to dissipate internally generated heat, and therefore the RTV interface curve was used for the PANSAT electronics box mounting conductances. The actual perimeter bolt patterns were estimated and can be modified if required.

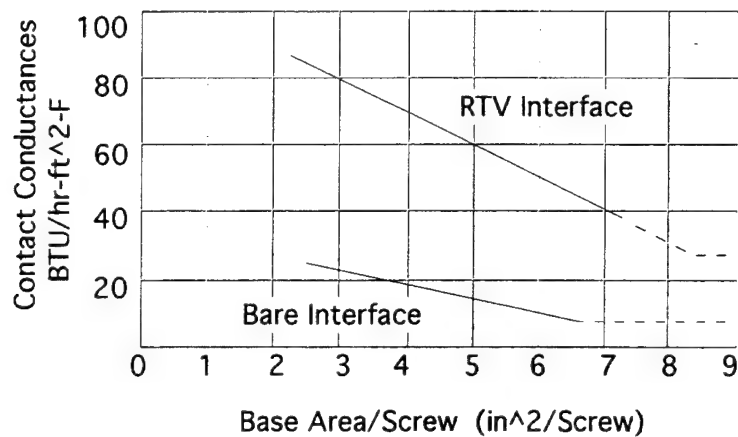


Figure 11. Empirically Derived Contact Conductances

Table 5 gives the contact conductances used in the PANSAT model for mounting electronics components. If a box base, represented in the model as a single node, covers more surface area than represented by one node on the deck then several contact conductances are established to the appropriate nodes, as an example the RF communications box base, node 1020, physically sits on deck surfaces represented by nodes 1010, 1011, and 1015, so three separate conductance values are established, adding up to the total conductance of the box to the deck.

Box	Footprint	Mounting Screws	Total Conduct- ance BTU/Hr-F	Partial Conduct- ance BTU/Hr-F	From Node (Box)	To Node (Struct)
RF Comm	3.0 x 10.0	6	12.5	8.5	1020	1010
			-	2.0	1020	1011
			-	2.0	1020	1015
EPS Box	5.5 x 6.0	8	14.9	-	2028	2018
DCS	8.25 x 11.0	8	5.0	1	2030	2018
			-	1	2030	2020
			-	1	2030	2022
			-	1	2030	2024

			-	1	2030	2026
Battery A	6.38 x 3.37	6	11.2	7	2034	2010
			-	2.1	2034	2011
			-	2.1	2034	2017
Battery B	6.38 x 3.37	6	11.2	7	2032	2014
			-	2.1	2032	2013
			-	2.1	2032	2015

Table 5. Electronics Box Mounting Contact Conductances

All the linear conductances used in the PANSAT are two way conductances allowing heat flow in either direction based on the thermal gradients. All conductance values are listed in Appendix C.

III. MODEL EVALUATION

A. ANALYTICAL THERMAL MODEL SOLUTION

Once all relevant data that describes the thermal characteristics of the PANSAT spacecraft is loaded into the ITAS environment, ITAS solution sequences can be executed and numerical analyses performed. The most significant results from the analyses are temperatures for various components. Both steady state and transient temperatures are available for all thermal nodes in the model, with the exception of the space sink node that remains at a constant -460°F. Intermediate data generated during solution sequences is also available for review (view factors, incident flux, absorbed heat rates), and serves to verify that results are correct.

The model that represents the PANSAT satellite is actually a composite of four individual models. Three separate sub-enclosures were generated to represent the three internal cavities in the spacecraft. These three sub-enclosure models were used to generate radiation interchange factors for the internal surfaces. These matrices were stored as separate files for use later. A model that represents the external geometry is used for the steady state and transient analyses. This external model also calls in the radiation interchange matrices developed for the sub-enclosures. All the pertinent user generated files are identified in Appendix B. Appropriate linear conductances are defined in the external model and used to link the internal geometry, and any relevant properties such as thermal dissipations and thermal mass, to the external geometry.

The analysis performed for both the steady state and the transient solutions is a matrix version of the following nodal heat balance equation [Reference 9],

$$\begin{aligned} m_i c_i \frac{dT_i}{dt} + \sum_{j=1}^n C_{ij} (T_i - T_j) + \sum_{j=1}^{n+1} \sigma R_{ij} (T_i^4 - T_j^4) \\ = P_i + \alpha_{si} A_i \mu_i S + \alpha_i A_i \phi_{Ai} + \epsilon_i A_i \phi_{Ti} \end{aligned} \quad (5)$$

Where,

- $m_i c_i$ = capacity of node i
- T_i, T_j = Temperatures of nodes i and j
- $\frac{dT_i}{dt}$ = Rate of temperature variation of node i
- C_{ij} = Conductive coupling between nodes i and j
- R_{ij} = Radiative coupling between nodes i and j
- P_i = Internal power dissipation of node i
- α_{si} = Solar absorptivity of node i
- ϵ_i = Emissivity of node i
- A_i = Area of radiation of node i
- μ_i = Solar aspect coefficient of node i
- S = Solar flux incident on node i
- ϕ_{Ai} = Albedo flux incident on node i
- ϕ_{Ti} = Earth radiation incident on node i

Steady state orbital temperatures are calculated by performing an energy balance at eight positions during the orbit. The individual temperatures are calculated according to Equation (5), setting the time dependent terms to zero, and then averaged. The solution takes into account environmental factors (incident flux, eclipse) as well as the internal thermal loads. The steady state temperatures give an averaged indication of the thermal balance for a specific node and is of less use than a full time history of the node. One additional problem is that since the steady state solution uses a very small number of positions for averaging the results are somewhat inaccurate. A better approach to determining steady state temperatures involves taking all detailed results from the transient runs and averaging them external to ITAS.

The transient analyses requires solving the time dependent version of Equation (5). The number of time steps used in the calculation is set by the user. The solution must be run for several orbits to establish an equilibrium in the energy balance. Once equilibrium is achieved the plot for any node will start and end at roughly the same temperature over an orbit period (some rounding errors do occur).

B. RESULTS

The number of parameters that have an impact on the thermal behavior of the PANSAT satellite is great. The list includes: seasonal variances in the environmental loads, absorptance and emittance of every surface, the parameters defining the orbit, the attitude of the spacecraft, all of the linear conductances that define relationships between the nodes, and the power dissipations of internal components. Establishing a matrix of solutions that would identify every possible combination of parameters would result in a cumbersome and useless data set. Instead the attempt was made to identify the two worst hot and cold cases that could occur on-orbit. This was done by running a series of test cases and selecting the most extreme cases. Detailed results are provided for the worst case hot and cold cases.

In addition to the developing detailed worst case results, an attempt is made to parameterize the variables that impact thermal performance and develop a set of sensitivity curves that demonstrate the influence individual variables have on PANSAT performance.

The operational requirements of the standard military electronics require that they be maintained within -67°F to 257°F (MIL-M-38510). Box baseplates generally have tighter requirements, more like -4°F to 140°F . and some components, like batteries, may have an operational temperature range that is even tighter.

1. Hot Case

The PANSAT analytical thermal model is used to predict the hottest possible temperatures based on the following assumptions:

Environmental Loads:		
	Solar Flux:	452.6 BTU/hr-ft ²
	Albedo:	0.3
	Earth IR:	87.2 BTU/hr-ft ²
Internal Dissipations:		
	RCM:	8 W
	EPS:	5 W
	DCM:	3 W
	Battery A:	5 W
	Battery B:	0 W
Orbital Parameters:		
	Orbit Altitude:	260 nm
	Orbit Inclination:	28.5°
	Longitude Of	
	Ascending Node:	180°
	Sun Declination:	23.45°

Table 6. Hot Case Parameters

The nodal parameters such as thermal mass, surface optical properties, and conductances, are given in Appendix C. At 480 km the orbit period is 94.2 minutes, including an eclipse period of approximately 27.9 minutes (with the hot case ephemeris). The environmental inputs are derived from Reference 10. The spacecraft attitude is earth pointing with the -X axis of the vehicle oriented towards the earth and the Y axis normal to the orbit plane (**Figure 12**). A table of hot case steady state temperature for every node is given in Appendix D.

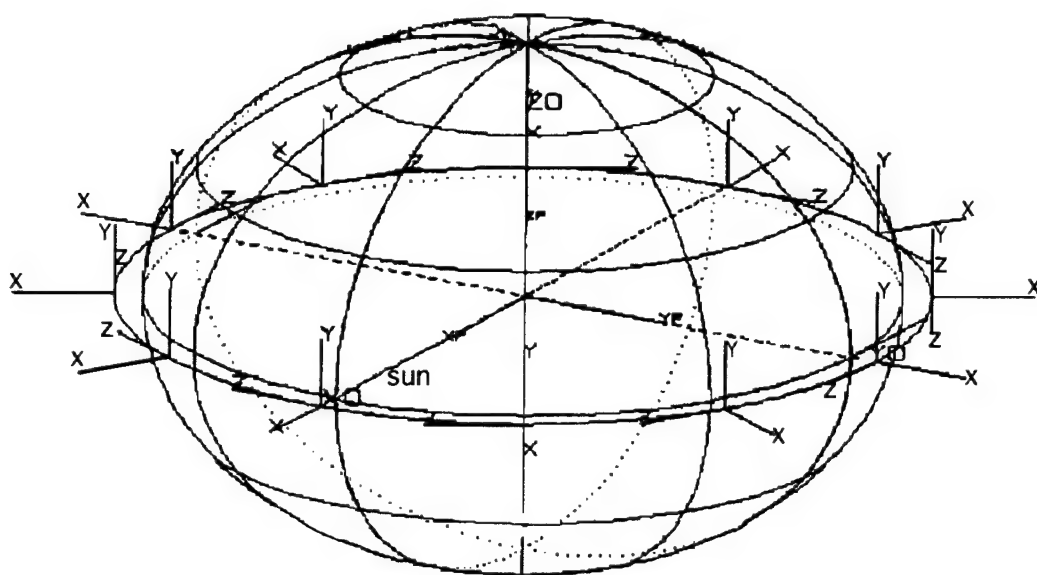


Figure 12. Hot Case Orbit

Figure 13 shows the fluctuation in component temperatures over one orbit period. The highest temperature recorded is 54°F for battery A. Battery B and the DCM box follow the same profile as Battery A since they are all mounted to the same deck. The DCM box is also dissipating heat and is therefore running a little warmer than battery B. The RFCM and the EPM boxes, which are both mounted on the upper equipment deck track the same temperature profile.

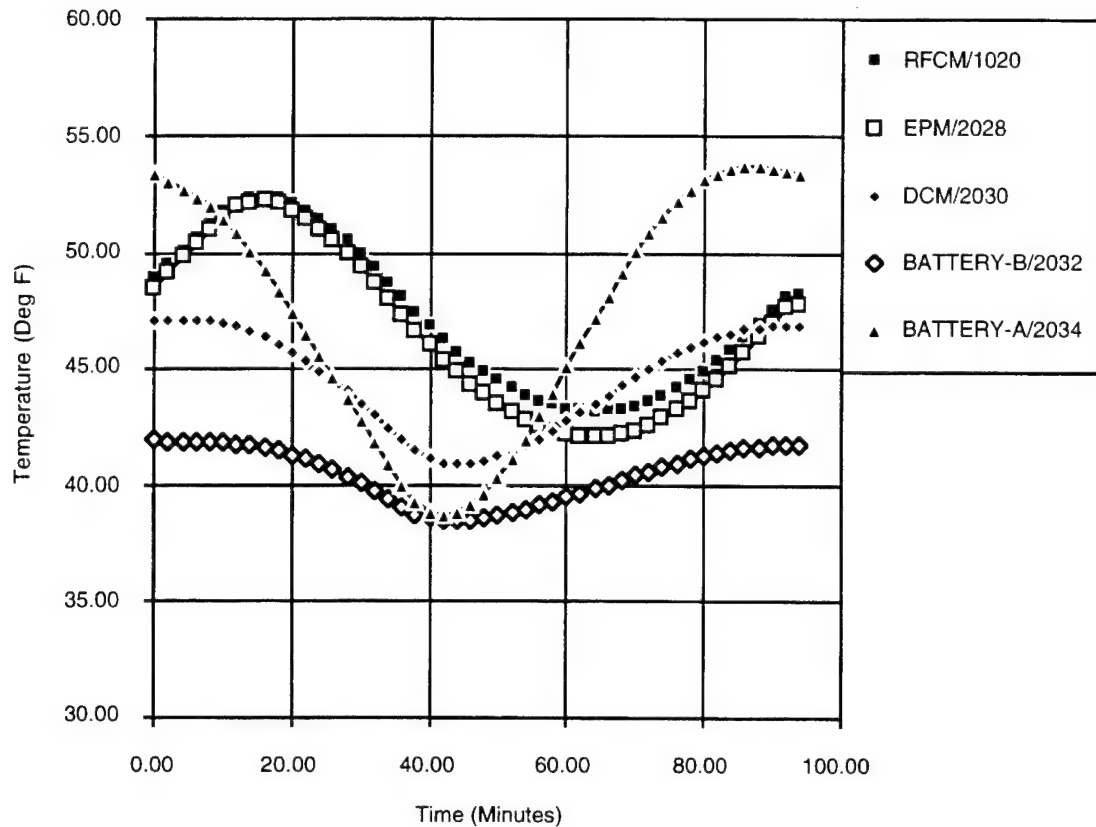


Figure 13. Electronics Box Temperatures - Hot Case

The relationship between the external surfaces and the internal components is highlighted in **Figure 14**. The external solar array nodes (nodes 18 and 20), will fluctuate much more widely than the internal node representing the RFCM box. Both external nodes are connected to the sub-enclosure model that represents the upper equipment bay which houses the RFCM electronics box. All three nodes track the same profile as would be expected for components on the +Z side of PANSAT. Eclipse starts about 10 minutes into this orbit cycle and the temperatures of the nodes pictured tend to drop. About 27 minutes later the satellite exits eclipse, but the +Z side of the spacecraft is being shadowed by the rest of the spacecraft body so any warming is due to radiative and conductive coupling with the rest of the spacecraft.

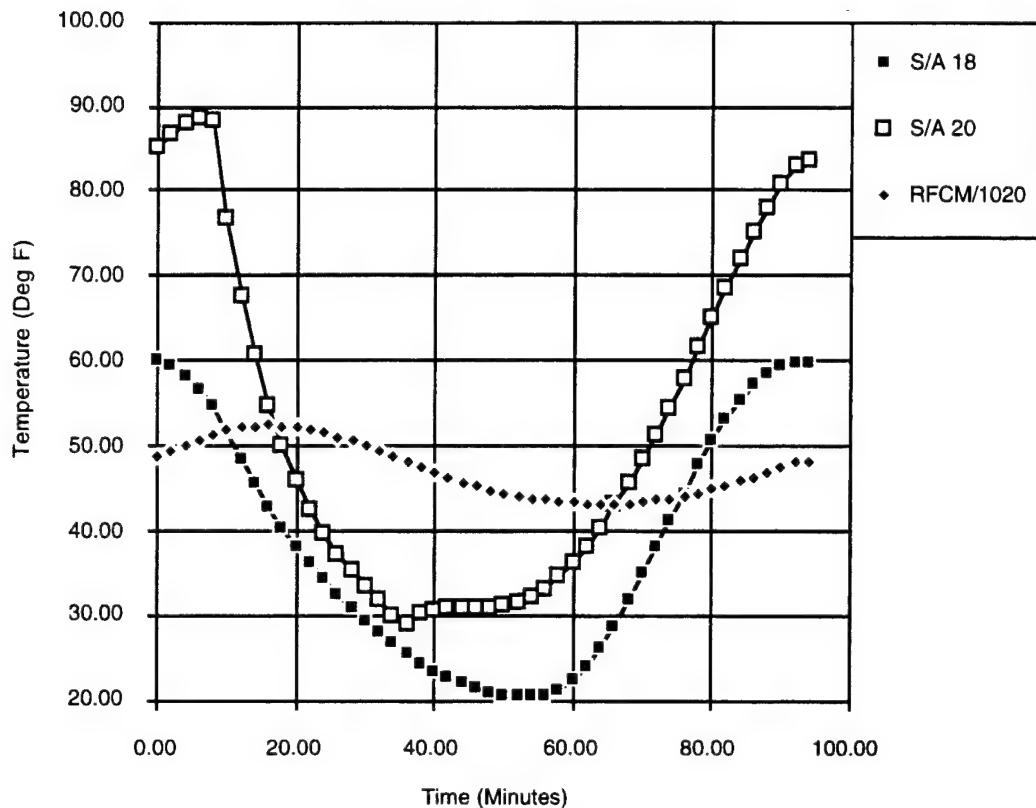


Figure 14. Solar Array Panel And RFCM Box Temperatures - Hot Case

The same solar array nodes are shown again in **Figure 15**. The RFCM node is replaced by another solar array node, but this one is on the -Z side of the spacecraft. Solar array node two is illuminated as soon as the spacecraft exits eclipse, about 37 minutes into this orbit cycle. Its temperature immediately begins to rise immediately. This again is due to the fact that it is being directly illuminated by the sun, but also because it has no contact (radiative nor conductive) with any internal dissipating masses. This demonstrates that light weight components, or components that are not linked to more massive, possibly heat dissipating sources, are more responsive to environmental changes.

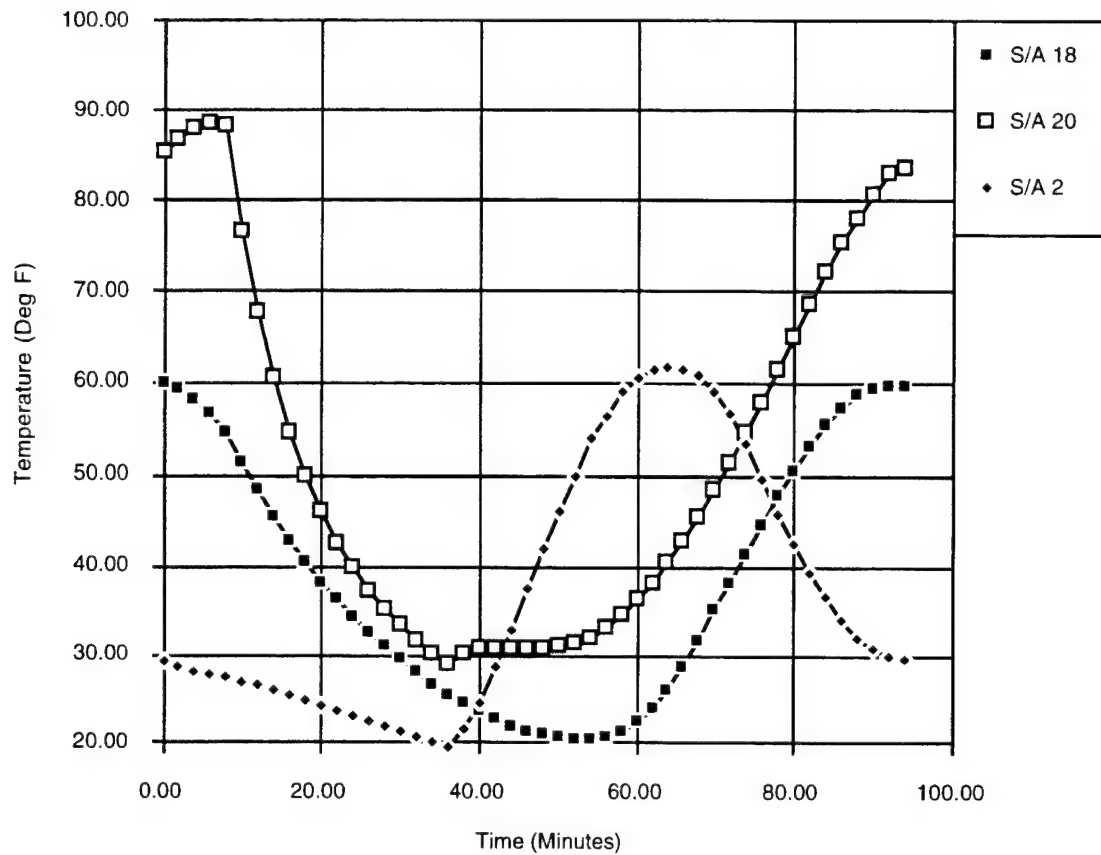


Figure 15. Solar Array Panel Temperatures - Hot Case

The equipment decks were discretized into several nodes due to their potential to not be isothermal. **Figure 16** shows several nodes from the upper equipment deck together. Although all the nodes behave similarly, as is expected, there is a slight temperature difference between them, and they are not isothermal. The accuracy of a model is largely determined by how isothermal the nodes which are used to discretize a system actually are [Reference 11].

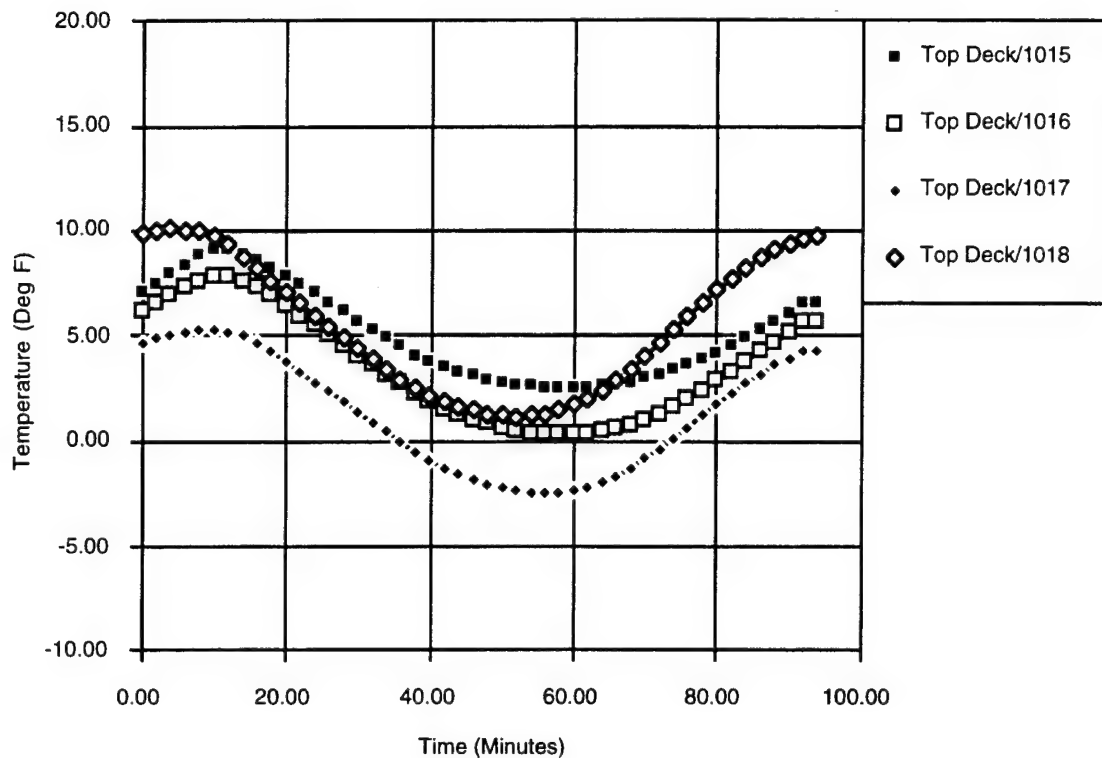


Figure 16. Upper Deck Nodes

2. Cold Case

The PANSAT analytical thermal model is used to predict the coldest possible temperatures based on the following assumptions:

Environmental Loads:		
Solar Flux:		417.12 BTU/hr-ft ²
Albedo:		0.125
Earth IR:		71.0 BTU/hr-ft ²
Internal Dissipations:		
RCM:		4W
EPS:		2 W
DCM:		1 W
Battery A:		2 W
Battery B:		0 W

Orbital Parameters:		
Orbit Altitude:	260 nm	
Orbit Inclination:	28.5°	
Longitude Of		
Ascending Node:	0°	
Sun Declination:	-23.45°	

Table 7. Cold Case Parameters

At 480 km the orbit period is 94.2 minutes, including an eclipse period of approximately 35.8 minutes (with the cold case ephemeris). The environmental inputs are derived from Reference 10. The same attitude is used in the cold case as in the hot case. A table of cold case steady state temperature for every node is given in Appendix D. **Figure 17** shows the fluctuation in component temperatures over one orbit period. The lowest temperature recorded is 5°F for battery A.

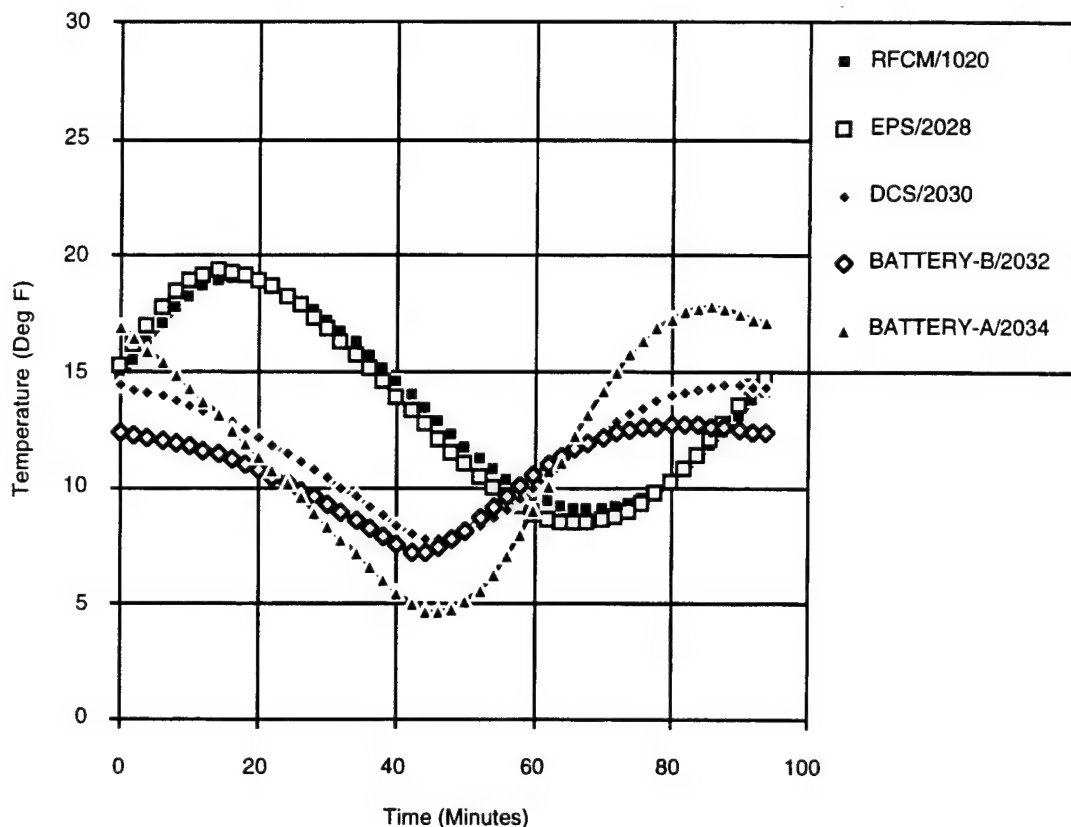


Figure 17. Electronics Box Temperatures - Cold Case

Figure 18 highlights the temperature differences between the hot case and the cold case. The internal electronics boxes are relatively sheltered from the external environment. They react primarily to the overall energy balance of the vehicle. The temperature history of the EPS box (node 2028) in both the hot and cold case is smooth. The overall shape of the curve is common to both cases, however there is a greater than 30°F offset between the two. The largest excursion the EPS box could expect to see is from +52°F (hot case high) to +9°F (cold case low). The history of an external panel in both the hot case and cold case is also given in **Figure 18**.

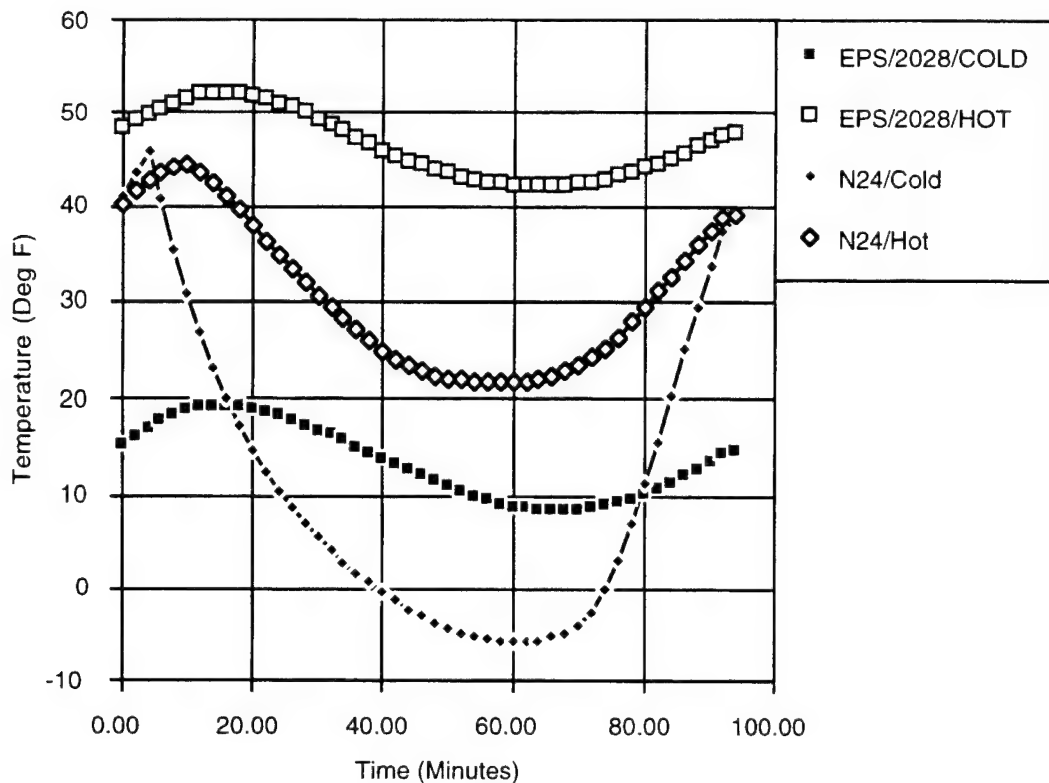


Figure 18. Comparison Of Hot Case And Cold Case

In addition to the steady state temperatures, Appendix D identifies the temperature extremes seen by every node in the thermal model in both the hot case and cold case.

3. Sensitivity Studies

In addition to determining absolute temperatures of the PANSAT spacecraft components, it is also helpful to develop an understanding of how sensitive the system is to specific parameters. The dominant thermal inputs to the PANSAT satellite are the environmental fluxes, not the internal dissipations. The amount of environmental flux absorbed, and internal heat dissipated, is dependent on the surface properties of the external structure. Of some concern is the fact that the external surfaces tend to degrade through time due to various effects, including atomic oxygen erosion, radiation effect, and thermal cycling. **Figures 19 and 20** show the impact of changing the absorptivity (α) and emissivity (ϵ) of the solar arrays. The nominal values are $\alpha=0.790$ and $\epsilon=0.85$ for the

solar arrays. In **Figure 19** the emissivity is held constant at 0.85 and the absorptance varied up and down 10% and 20% from the nominal 0.790 value. In **Figure 20** the absorptance is held at the nominal value and the emissivity varied up and down 10% and 20%. The curves demonstrate how changing the values by a relatively small percent either up or down, can cause a fairly dramatic change in temperatures. The effect seems to be fairly linear. Both the external array surface (node 9) and an internal electronics box (RFCM, node 1020) are effected by changes in the surface properties of external nodes.

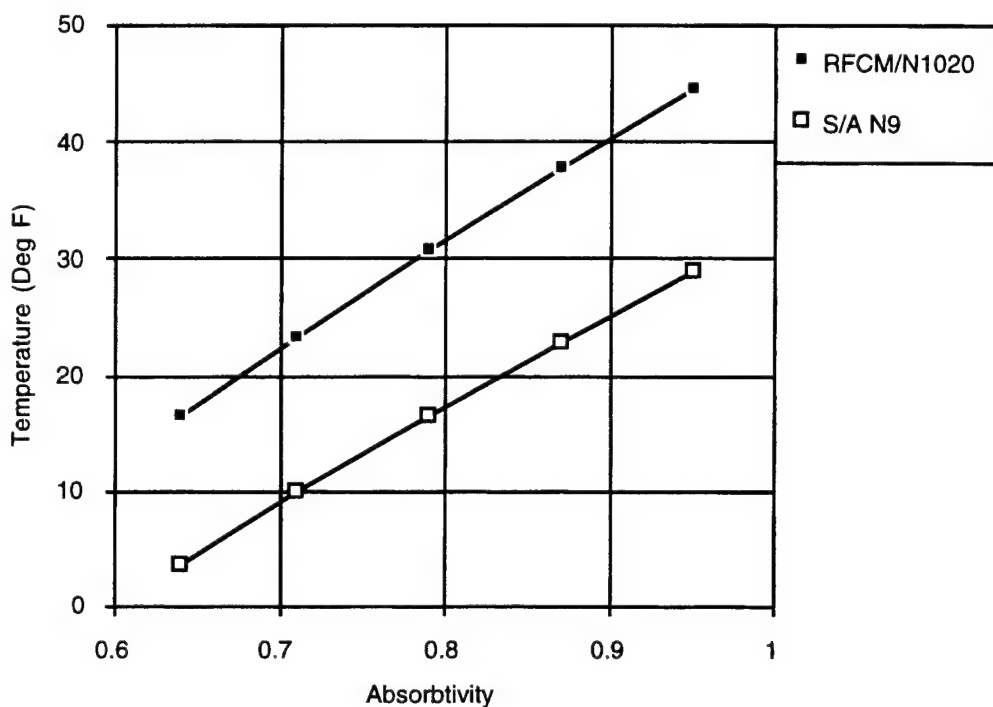


Figure 19. Temperature Sensitivity To Solar array Absorptivity

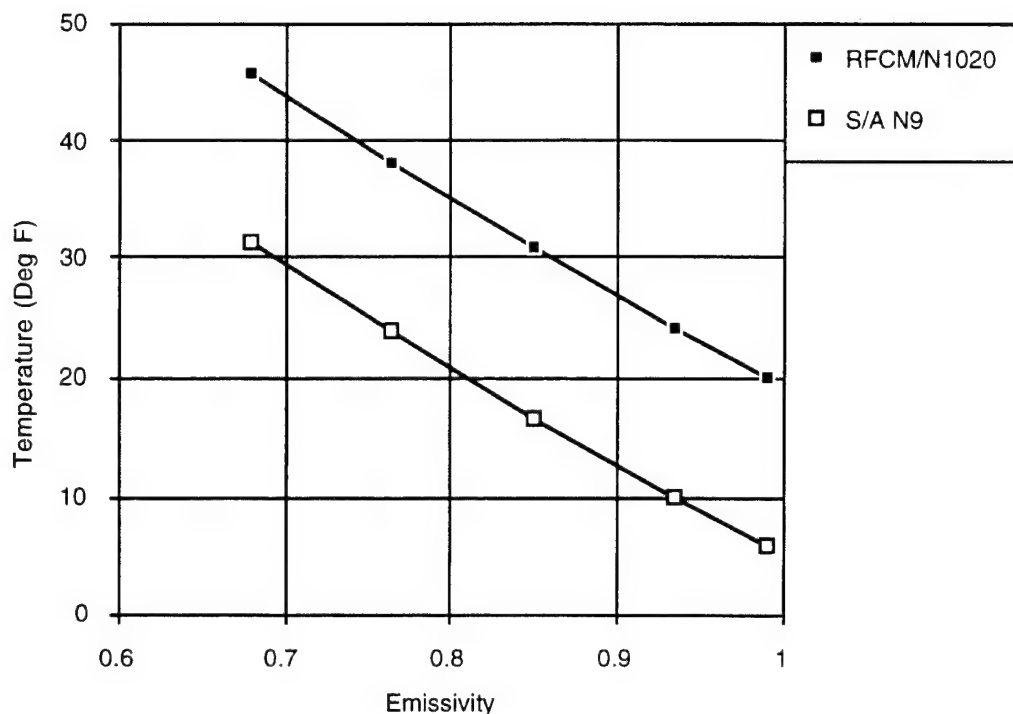


Figure 20. Temperature Sensitivity To Solar Array Emissivity

The other exposed surfaces on the PANSAT satellite are the triangular closeout panels. These eight panels were initially modeled as bare (solvent wiped) aluminum ($\alpha=0.16$ and $\epsilon=0.70$). The surface properties of the aluminum may degrade through time, but more significantly these panels can be used as a design parameter for initially setting the average temperature of the spacecraft of a desired level. Although these triangular panels account for a small percentage (<20%) of the total surface area of the vehicle, modifying the surface properties of these components does have a significant impact on both their temperature and on the temperature of internal components. Changing either the emissivity or absorptance individually by a factor of two will change the average temperature of internal components by more than 5°F, as shown in **Figure 21** and **Figure 22**.

Another parameter that is expected to have an impact on the thermal environment of a spacecraft is the vehicle attitude. In the case of PANSAT, the fixed geometry and uniform

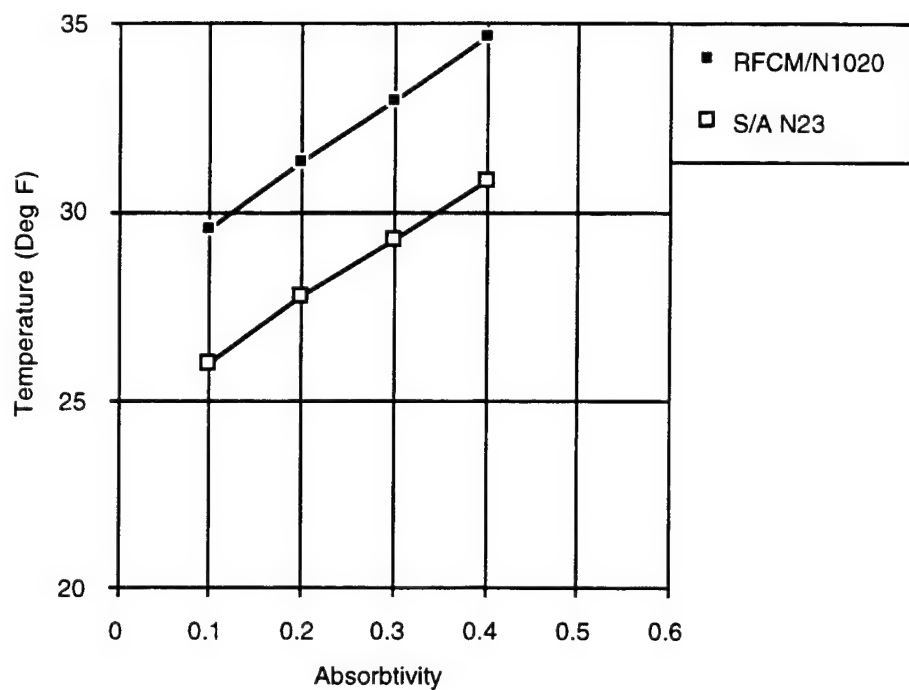


Figure 21. Temperature Sensitivity To Triangular Panel Absorptivity

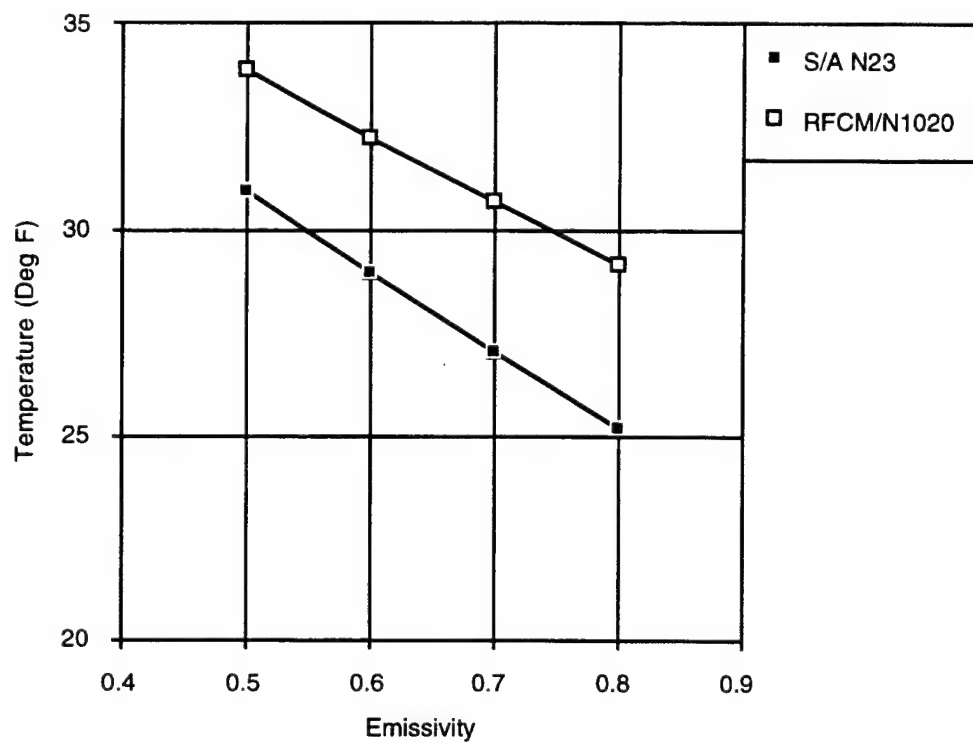


Figure 22. Temperature Sensitivity To Triangular Panel Emissivity

distribution of surface properties results in vehicle attitude not having a significant impact on the system. In an orbit where the vehicle establishes an earth facing side and maintains it through the orbit there is some variance in internal component temperatures based on which side is earth facing. This is primarily a result of the fact that the internal distribution of electronics is not uniform, some components have a good view of the solar arrays and closeout panels, others such as the DCS views equipment deck surfaces and other boxes primarily. **Figure 23** highlights this point by plotting temperature profiles of the same node in two runs where the only difference is the attitude. The vehicle was set in an earth facing orientation with the X axis nadir pointing. The vehicle was rotated about the X axis by 90 degrees between runs. Temperature profile change is only about 4°F. External surface temperatures do vary significantly based on attitude. In one orientation a surface may see the sun while in another orientation it is blocked from the sun by the rest of the spacecraft. The important feature is that while individual surfaces may see different temperature histories, the average system temperatures are not greatly affected by attitude. In a tumble mode where the vehicle rates ensure that there are no long term fixed orientations the temperature histories are even more uniform throughout the vehicle.

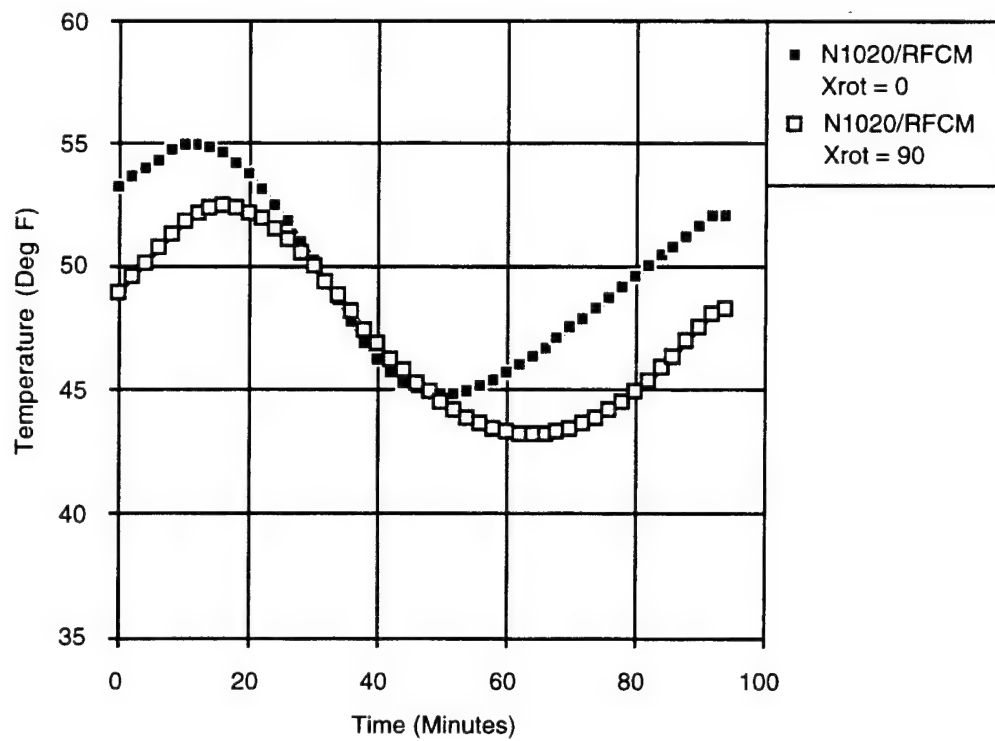


Figure 23. Internal Node Temperature For Two Different Attitudes

IV. PANSAT THERMAL TESTING

A. THERMAL TESTING IN THE DESIGN PROCESS

Spacecraft thermal design is an integrated, iterative process involving both analytical modeling and component and system level ground testing. Different types of thermal tests are used to verify the thermal design and ensure proper operation of all subsystems. The iterative relationship between testing and analysis (Figure 2) is intended to reduce risk and develop more confidence in the spacecraft thermal design prior to launch. The analytical model developed from this thesis will be used during system level thermal testing for the reasons described in the following sections.

Various standards, such as MIL-STD-1540 B [Reference 12] and MIL-STD-343 [Reference 13], attempt to define testing requirements in general terms. Both documents are intended to be used as reference guidelines. Program specific test philosophies are developed and implemented on a case by case basis to verify thermal designs in the most effective and efficient manner. This portion of the thesis is intended to outline required ground based system level thermal testing for the PANSAT program. A separate formal test plan document needs to be generated as well as detailed procedure for conducting the required tests. Component level testing will not be addressed as part of this thesis.

B. SYSTEM LEVEL THERMAL TESTING

1. Thermal Design Verification Test

The thermal design verification test (TDVT) - often referred to as the thermal balance test - is the first spacecraft thermal test performed at the system level. The primary purpose of the TDVT is to validate the analytical model. The test will also demonstrate the functional capability of any thermal control hardware. The test is preferably conducted after the first version of the analytical model is completed. The analytical model is run through a set of environmental and internal load cases that should cover all the possible situations that could be encountered on-orbit. The results of these

various conditions are evaluated and a set of worst case conditions that envelope the others, one extreme hot case and one extreme cold case, is identified. This set of loads becomes the basis for the TDVT.

Thermal loads used in the analytical model are based on the environment seen in space. Many organizations wish to validate the thermal design with ground testing by simulating these loads as closely as possible during testing. The problem with this approach is that it is inherently costly and potentially inaccurate. Specialized equipment such as collimated solar simulation lamps and IR radiating hot plates are required to produce the necessary environmental loads. The accuracy with which the environmental thermal inputs can be simulated is questionable. Accurately simulating the solar spectral distributions and solar beam collimating is difficult. Reflection and re-radiation are also possible error sources.

An alternative approach for test validation of a thermal model has been used at NRL in past programs. Instead of attempting to simulate in the physical world the exact load conditions used in the on-orbit analytical model, another set of external fluxes is used that can be easily produced by available test fixtures and facilities. A set of electrical heater dissipations is applied to the analytical thermal model surfaces upon which are incident the various environmental fluxes to match the predicted flux absorptions based on surface absorptances and emittance. Thus absorbed (solar and earth) fluxes are input both to the analytical test model and the actual surfaces on the test article in the form of electrical heater dissipations. No simplifications are required in the thermal model itself, only in the application of loads. This approach reduces the cost of the testing and eliminates possible error sources in the thermal inputs. **Figure 24** and **Figure 25** contrast the differences in the two approaches.

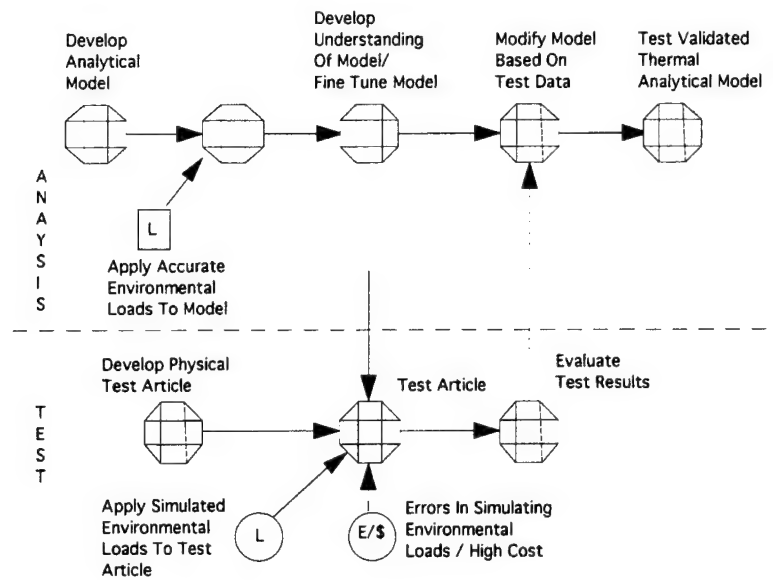


Figure 24. Conventional TDVT Approach Used For Model Validation

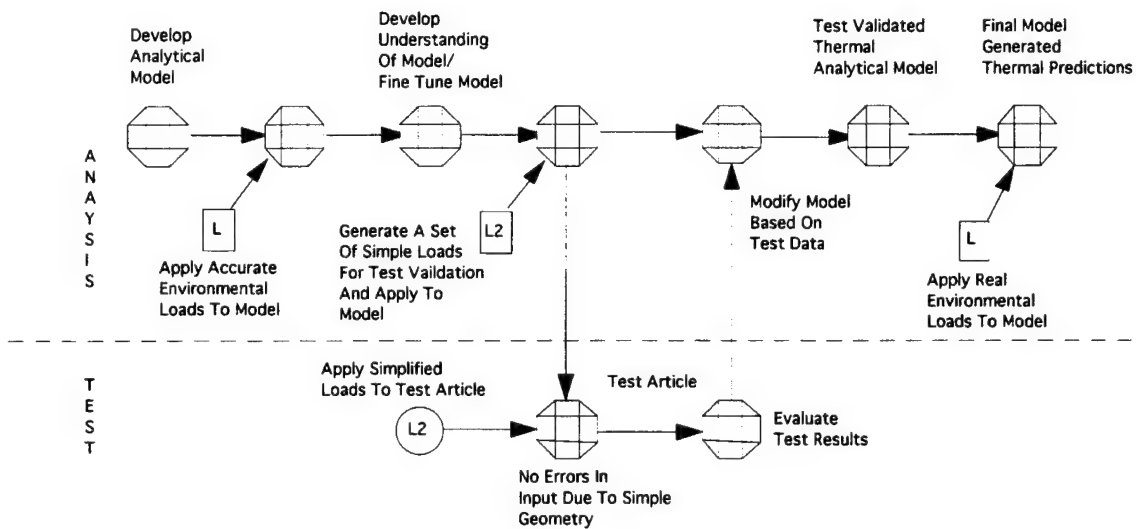


Figure 25. Improved TDVT Approach Used For Model Validation

In general, several configurations may also be tested but due to the spherical geometry of the PANSAT satellite only one hot and one cold case needs to be developed for the TDVT.

2. Thermal Vacuum Testing

System level thermal vacuum tests are intended to demonstrate performance of all subsystems at temperature extremes and in between. These tests verify proper interaction between components and subsystems. Test levels and durations depend on the type of testing being done, i.e. qualification or acceptance. Previously mentioned MIL-STD reference documents recommend margin on predicted temperature environments and number of cycles for various types of tests. Generally, qualification tests require a minimum of eight cycles with at least 10°C design margin at temperature extremes, acceptance tests require a minimum of four cycles with at least 5°C design margin at temperature extremes. Full functional checkouts are done before and after all tests. Spacecraft equipment is operated during testing as well.

3. PANSAT Testing

A test plan needs to be developed for PANSAT. Part of that document will pertain specifically to the required thermal testing. Both a TDVT and a thermal balance test should be conducted for the PANSAT system. Both tests could be conducted in the same facility. The TDVT should be conducted first. If the schedule permits, the test data should be fully analyzed and the analytical model could be updated prior to thermal vacuum testing. If this is not possible the TDVT could be performed just prior to the thermal vacuum testing without breaking the seal on the vacuum chamber. The environmental loads should be applied using surface mounted electrical heaters for the reasons described earlier. The loads applied to the external surfaces are derived from the analytical thermal model results. Table 8 provides the absorbed heat flow (averaged over the orbit) on the external nodes for the PANSAT model during the hot case (a similar table is required for the cold case. The internal dissipations should also be provided by electrical heaters. If the TDVT is combined with the system level thermal vacuum test then flight components can be used to provide internal dissipations. No system level thermal testing should be undertaken until the current analytical model is reviewed and

updated with the latest information regarding configuration, materials, and power dissipations thermal.

Node	UV (Btu/hr)	IR (Btu/hr)	Total (Btu/hr)
1	1.7	6.3	8.0
2	0.2	7.5	7.6
3	0.1	1.3	1.4
4	1.7	16.1	17.8
5	1.1	0.8	2.0
6	4.1	4.6	8.7
7	1.1	0.1	1.2
8	1.7	0.5	2.2
9	0.1	0.0	0.1
10	0.0	7.6	7.6
11	0.2	17.6	17.8
12	1.8	22.6	24.4
13	3.7	11.3	15.0
14	5.6	3.4	9.0
15	3.7	1.2	4.8
16	1.8	0.5	2.3
17	0.2	0.0	0.2
18	0.2	7.5	7.6
19	0.1	1.3	1.4
20	1.7	16.1	17.8
21	1.1	0.8	2.0
22	4.1	4.6	8.7
23	1.1	0.1	1.2
24	1.7	0.5	2.2
25	0.1	0.0	0.1
26	1.9	7.1	9.0

Table 8. Averaged Environmental Absorbed Heat Flow For The Hot Case

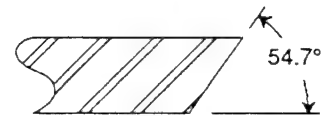
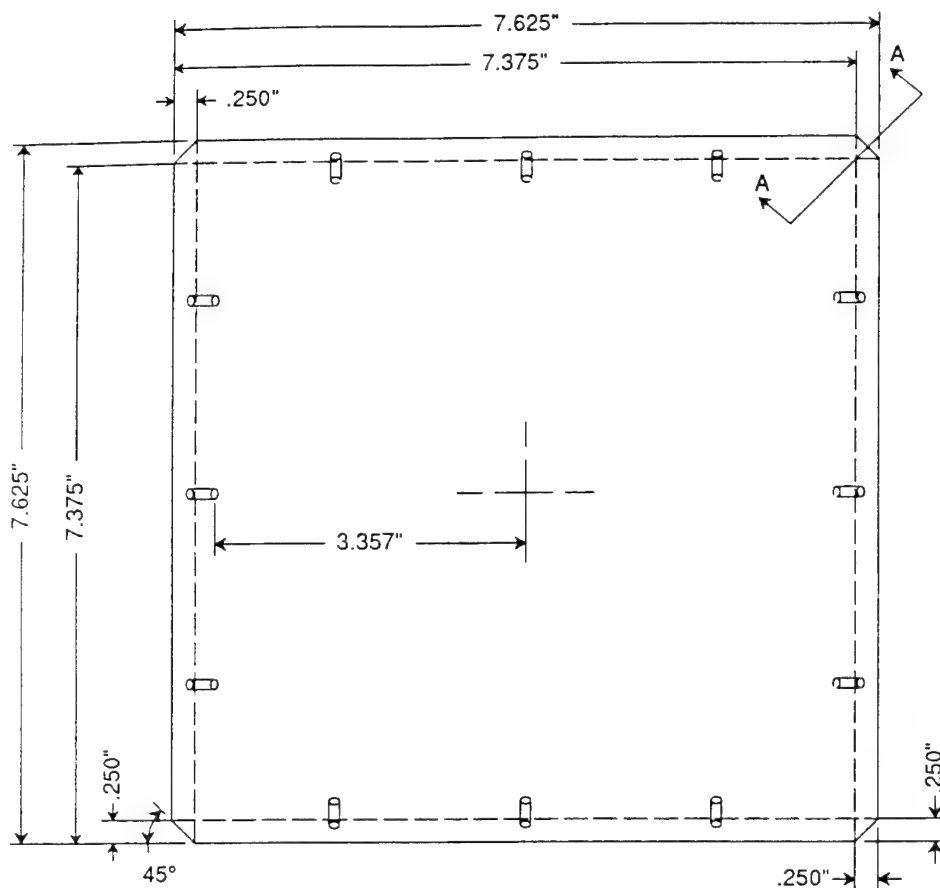
V. CONCLUSIONS

An analytical thermal model of the PANSAT satellite has been successfully developed. The model has been evaluated using a variety of loading conditions and environments. A single worst case hot case and cold case have been identified. The analytical model shows that the preliminary all passive thermal design is adequate for the predicted loads and environments in these extreme cases. Model results include steady state temperatures and maximum/minimum temperatures for every node in the model (Appendix D). In addition, several parametric studies were made to determine the sensitivity of the design to changes in identified parameters (solar array absorbtance and emittance, spacecraft attitude).

Some assumptions were made in creating the analytical thermal model (number of fasteners per box, RTV used for box mounting). Once these assumptions are verified this model can be used to support the system level thermal testing that is required for the PANSAT program.

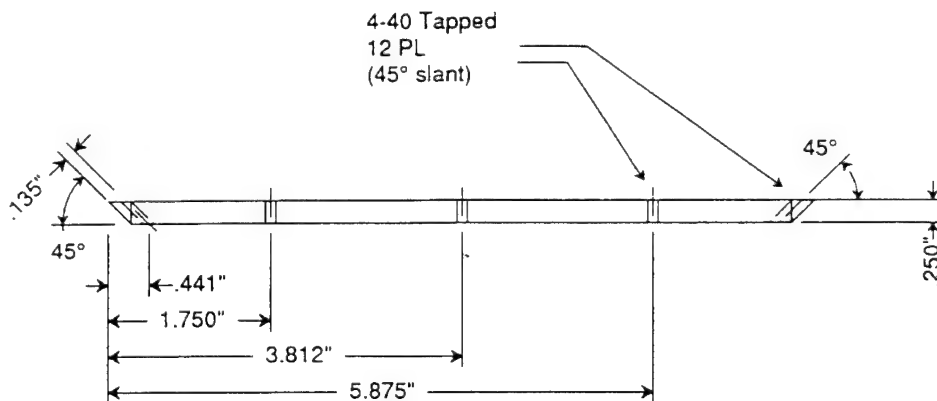
APPENDIX A

This Appendix provides drawings of all structural components used in the development of the PANSAT analytical thermal model.



View 'A'

Angle cut at all (4) corners is 54.7°



Use Aluminum 6061-T6
(1) Required

All Dimensions in Inches

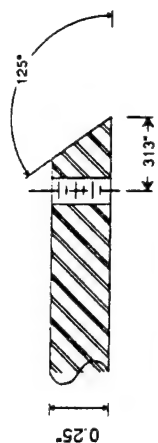
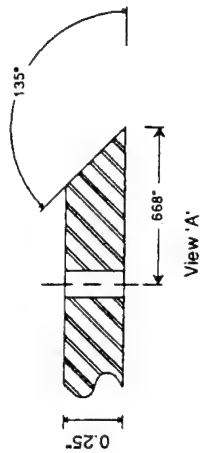
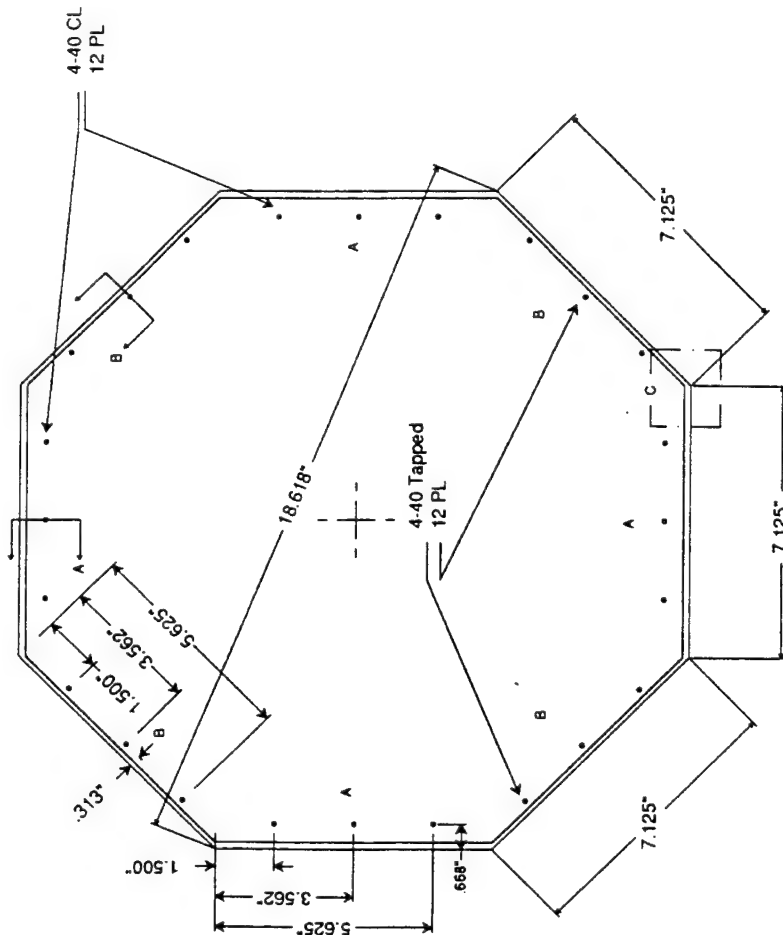
REVISION LTR	DATE	DEPARTMENT OF THE NAVY	SPACE SYSTEMS ACADEMIC GROUP
	DATE	NAVAL POSTGRADUATE SCHOOL	MONTEREY, CALIFORNIA
	DATE	PANSAT TOP PLATE	
	DATE		
DRAWN BY: D. Sakoda	DATE 14 May 91		
APPROVED BY:	DATE	DRAWING NO. TOP PLATE	SHEET 1 OF 1

Aluminum 6061-T6
(4) Required

REVISION	LTR
A	1.164"
B	0.707"
C	0.500"

All Dimensions in Inches

REVISION LTR	DEPARTMENT OF THE NAVY	SPACE SYSTEMS ACADEMIC GROUP
DATE	NAVAL POSTGRADUATE SCHOOL	
DATE	MONTEREY, CALIFORNIA	
DATE	PANSAT TOP PANEL	
DATE		
DATE		
DATE		
DRAWN BY D. SAKODA	DRAWING NO	Top Panel
APPROVED BY	DATE 14 May 91	SHEET 1 OF 1



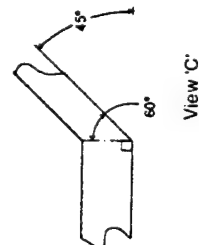
View 'B'

Edge angles alternate between 135° and 125° about the plate as shown. 'A' sides are not tapped 'B' sides have 4-40 CoilThread Inserts

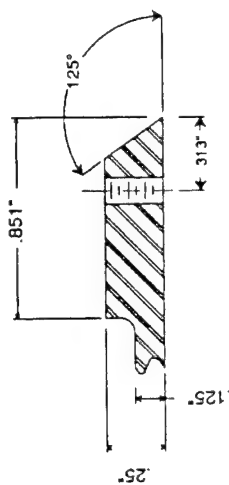
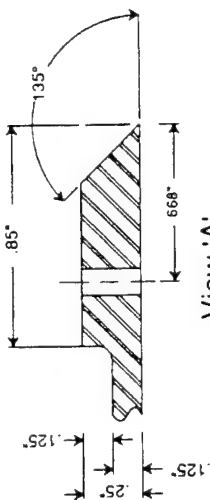
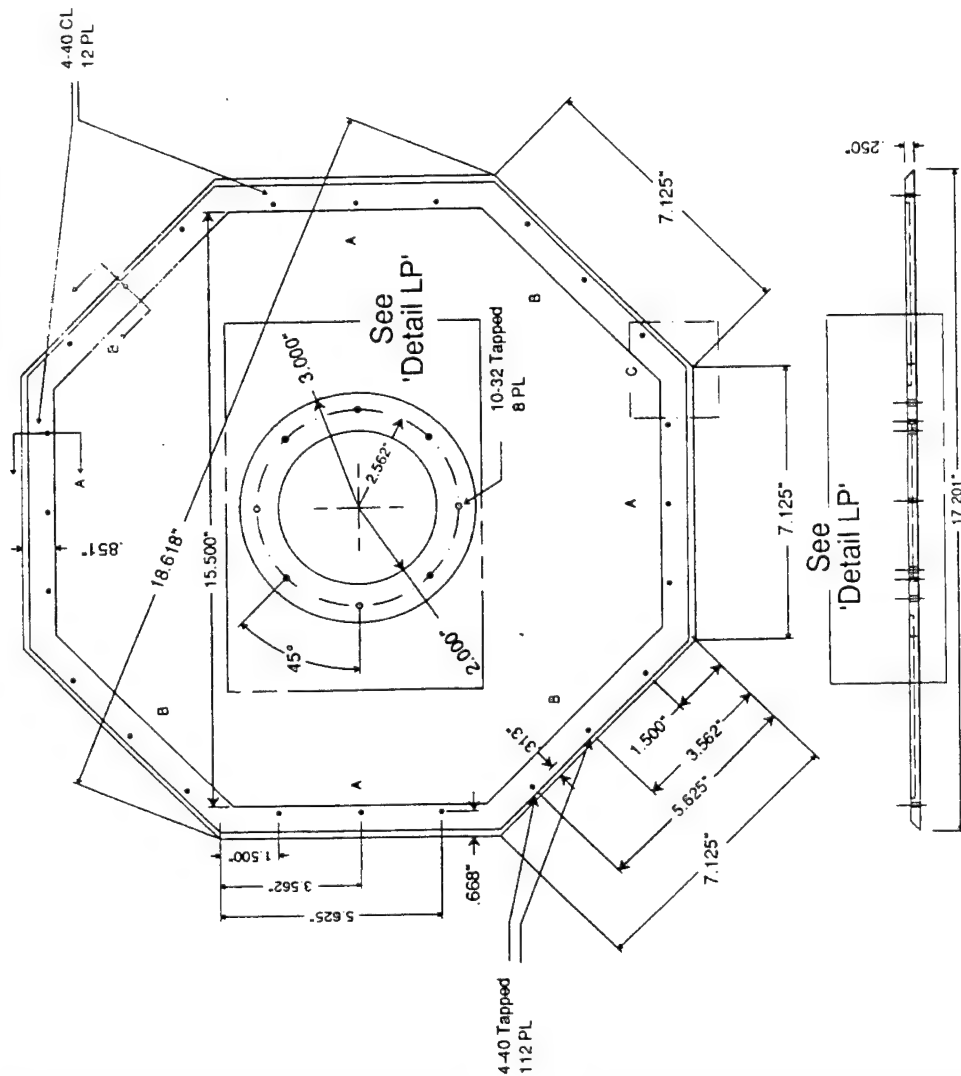
Use Aluminum 6061-T6
(1) required

All Dimensions in Inches

REVISION/LTR	DATE	DEPARTMENT OF THE NAVY	SPACE SYSTEMS ACADEMIC GROUP
	DATE	NAVAL POSTGRADUATE SCHOOL	MONTEREY, CALIFORNIA
	DATE	PANSAT UPPER EQUIPMENT PLATE	
	DATE		
DRAWN BY:	DATE	DRAWING NO	SHEET 1 OF 1
D. Sakoda	14 May 91	UPPER PLATE	
APPROVED BY:	DATE		



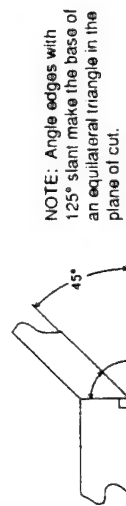
NOTE: Angle edges with 125° slant make the base of an equilateral triangle in the plane of cut.



View 'B'

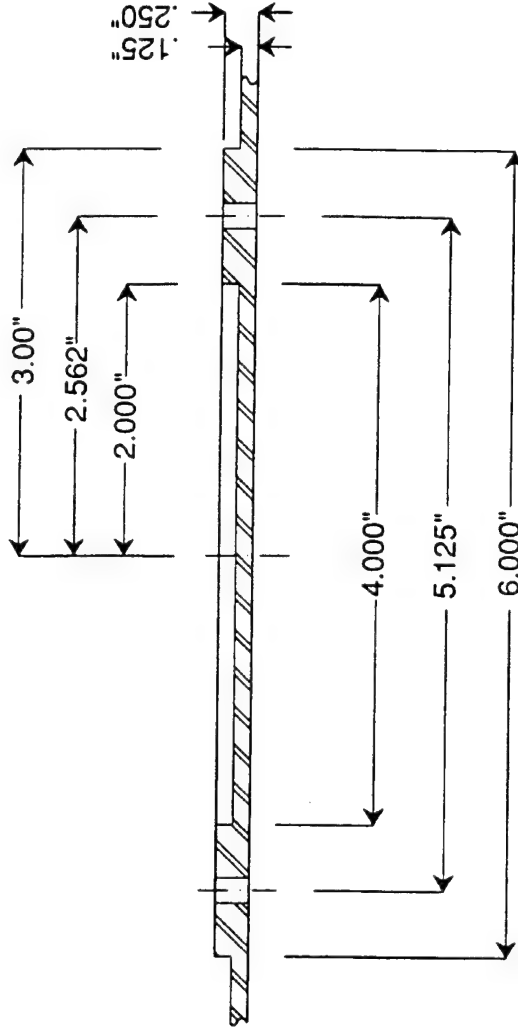
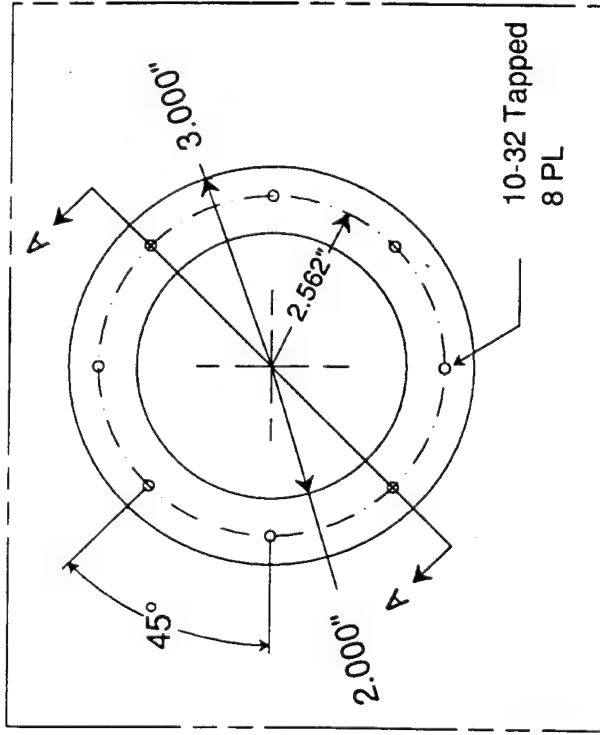
Edge angles alternate between 135° and 125° about the plate as shown.

All Dimensions in Inches

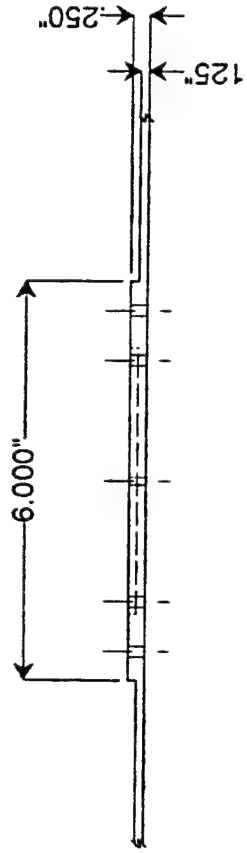


NOTE: Angle edges with 125° slant make the base of an equilateral triangle in the plane of cut.

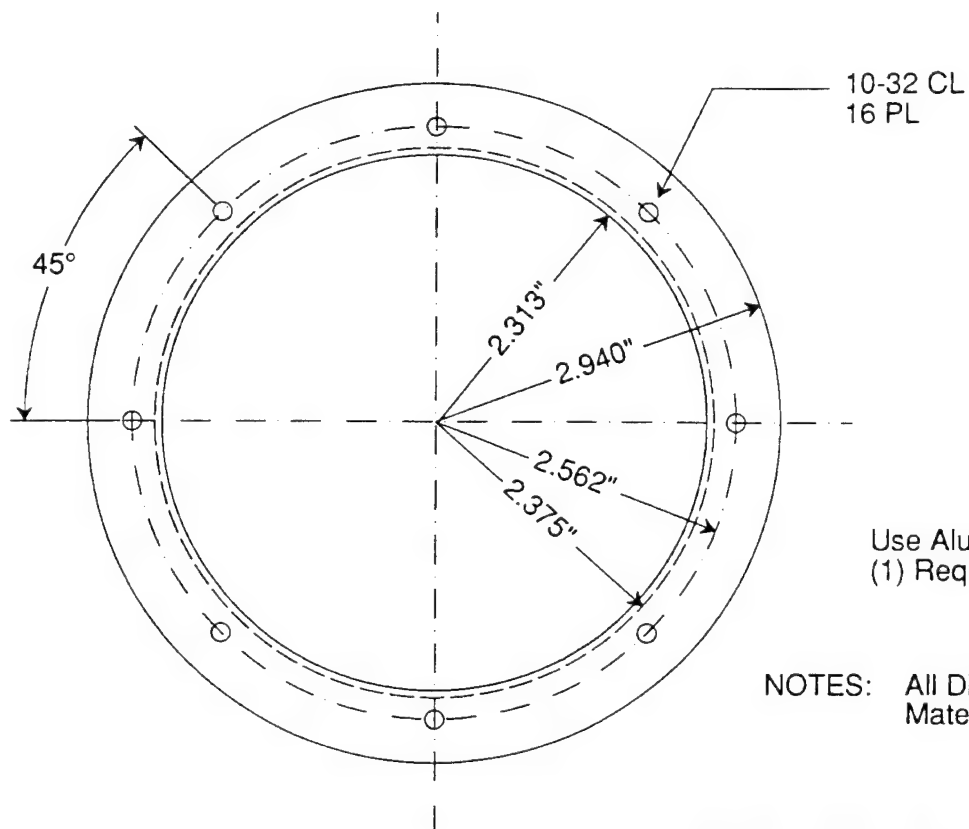
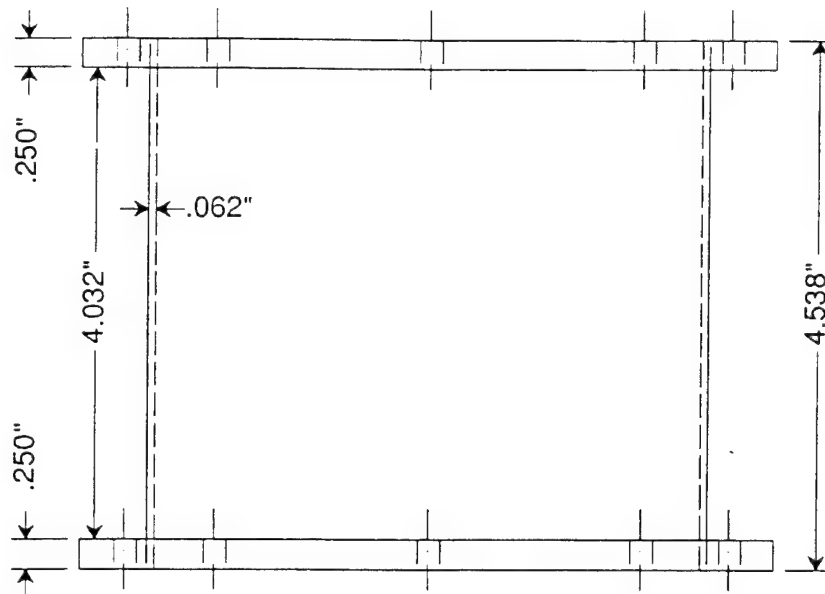
REVISION LTR	DATE	DEPARTMENT OF THE NAVY	SPACE SYSTEMS ACADEMIC GROUP
	DATE	NAVAL POSTGRADUATE SCHOOL	MONTEREY, CALIFORNIA
	DATE	PANSAT LOWER EQUIPMENT PLATE	
	DATE		
DRAWN BY:	DATE 14 May 91	Lower Plate	
D. Sakoda			
APPROVED BY	DATE	DRAWING NO.	SHEET 1 OF 2



View 'A'



REVISION LTR	DATE	DEPARTMENT OF THE NAVY	SPACE SYSTEMS ACADEMIC GROUP
	DATE	NAVAL POSTGRADUATE SCHOOL	MONTEREY, CALIFORNIA
	DATE	Detail LP (Lower Equipment Plate)	
	DATE		
DRAWN BY: D. Sakoda	DATE 17 Jan 91	DRAWING NO Detail LP SHEET 2 OF 2	
APPROVED BY:	DATE		

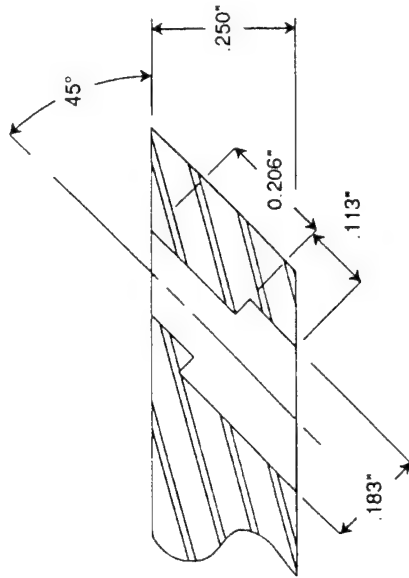
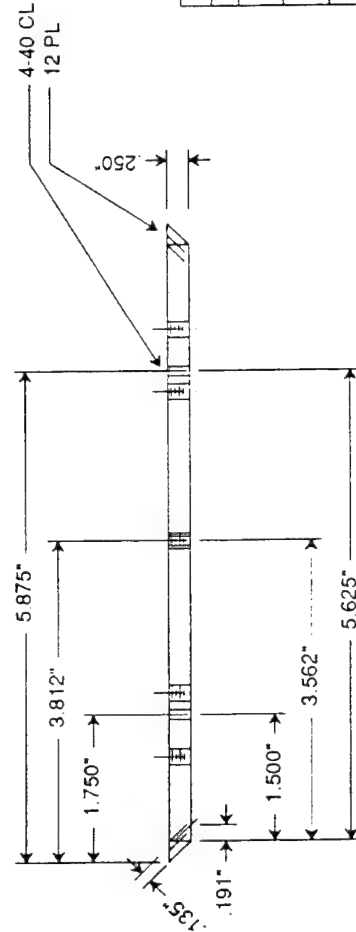
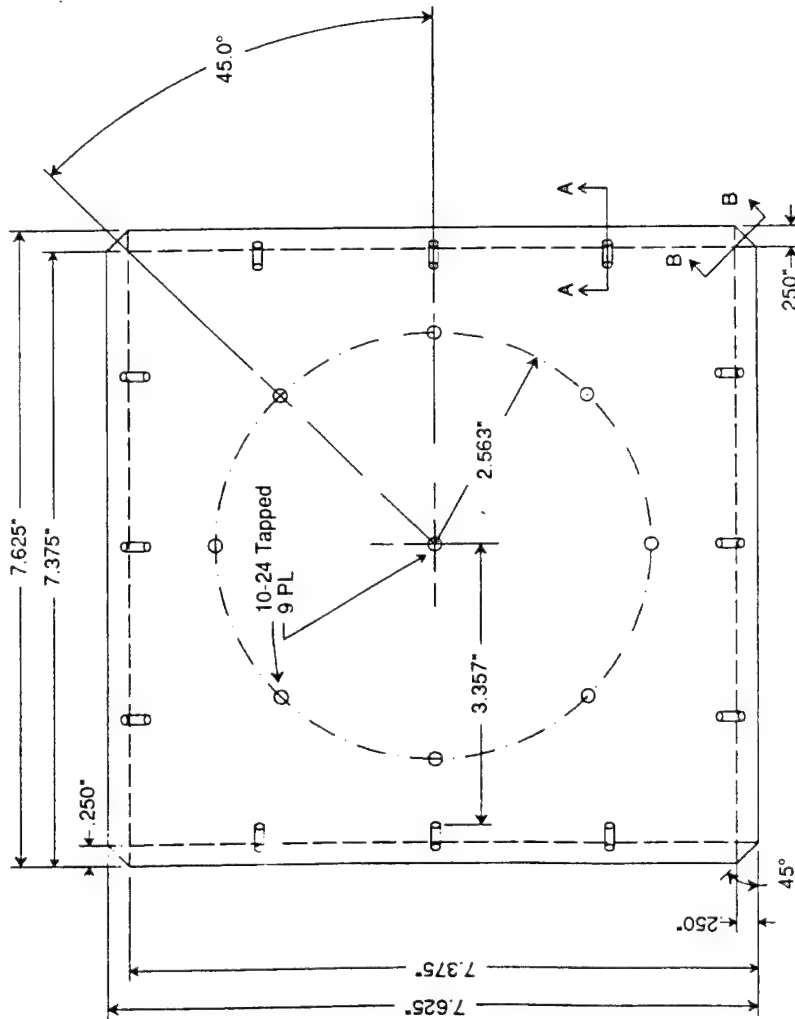


NOTES: All Dimensions in Inches
Material is Aluminum 6061-T6

REVISION LTR	DATE	DEPARTMENT OF THE NAVY	SPACE SYSTEMS & ACADEMIC GROUP
		NAVAL POSTGRADUATE SCHOOL	MONTREY, CALIFORNIA
		PANSAT SUPPORT CYLINDER	
DRAWN BY: D. Sakoda	DATE 16 Jan 91	DRAWING NO.	Base Cylinder
APPROVED BY:	DATE		SHEET 1 OF 1

[illegible]

REVISION LTR	DEPARTMENT OF THE NAVY	SPACE SYSTEMS ACADEMIC GROUP
DATE	NAVAL POSTGRADUATE SCHOOL	
DATE	MONTEREY, CALIFORNIA	
DATE	PANSAT BASE	
DATE	PANEL	
DRAWN BY: D SAKODA	DRAWING NO	SHEET 1 OF 2
APPROVED BY:	Bot Panel	



View 'A'



View 'B'

Angle cut at all (4) corners is 54.7°

REVISION/LTR	DATE	DEPARTMENT OF THE NAVY	SPACE SYSTEMS ACADEMIC GROUP
	DATE	NAVAL POSTGRADUATE SCHOOL	MONTEREY, CALIFORNIA
	DATE	PANSAT BASE PLATE	
	DATE		
DRAWN BY D Sakoda	DATE 15 May 91	DRAWING NO	BASE PLATE
APPROVED BY	DATE	SHEET 1 OF 1	

APPENDIX B

This Appendix provides a listing of all user generated files that are used in the hot and cold case steady state and transient analyses of the PANSAT analytical thermal model.

Hot Case:

SHELLH.INP	Geometry data file for external model
SHELLH.PIN	Parameter file for external model
SHELLH.VIU	View factor file for external model
SHELLH.SHD	Shadow factor file for external model
ENCLTOP.INP	Geometry data file for upper subenclosure model
ENCLTOP.PIN	Parameter file for upper subenclosure model
ENCLTOP.VIU	View factor file for upper subenclosure model
ENCLTOP.RAD	Radiation conductance file for upper subenclosure model
ENCLMID.INP	Geometry data file for middle subenclosure model
ENCLMID.PIN	Parameter file for middle subenclosure model
ENCLMID.VIU	View factor file for middle subenclosure model
ENCLMID.RAD	Radiation conductance file for middle subenclosure model
ENCLBOT2.INP	Geometry data file for bottom subenclosure model
ENCLBOT2.PIN	Parameter file for bottom subenclosure model
ENCLBOT2.VIU	View factor file for bottom subenclosure model
ENCLBOT2.RAD	Radiation conductance file for bottom subenclosure model
HOT1-6.DAT	Transient analysis results on orbits one through six
HOT7-10.DAT	Transient analysis results on orbits seven through ten
HOT11-14.DAT	Transient analysis results on orbits eleven through fourteen

Cold Case:

SHELLC.INP	Geometry data file for external model
SHELLC.PIN	Parameter file for external model
SHELLC.VIU	View factor file for external model
SHELLC.SHD	Shadow factor file for external model
ENCLTOP.INP	Geometry data file for upper subenclosure model
ENCLTOP.PIN	Parameter file for upper subenclosure model
ENCLTOP.VIU	View factor file for upper subenclosure model
ENCLTOP.RAD	Radiation conductance file for upper subenclosure model
ENCLMID.INP	Geometry data file for middle subenclosure model
ENCLMID.PIN	Parameter file for middle subenclosure model
ENCLMID.VIU	View factor file for middle subenclosure model
ENCLMID.RAD	Radiation conductance file for middle subenclosure model

ENCLBOT2.INP
ENCLBOT2.PIN
ENCLBOT2.VIU
ENCLBOT2.RAD

Geometry data file for bottom subenclosure model
Parameter file for bottom subenclosure model
View factor file for bottom subenclosure model
Radiation conductance file for bottom subenclosure model

COLD1-6.DAT
COLD7-12.DAT
HOT13-16.DAT

Transient analysis results on orbits one through six
Transient analysis results on orbits seven through twelve
Transient analysis results on orbits thirteen through sixteen

APPENDIX C

This Appendix provides an ITAS generated listing of all nodes and conductances in the PANSAT analytical thermal model. This data deck was run for the hot case.

PC-ITAS Node and Conductance Report

```
*****
Date: 02/02/95                      Time: 22:28:23.05
PC-ITAS Version Number: 9.2A        Release Date: DEC 7, 1994
*****
```

PC-ITAS SURFACE-to-NODE & Properties

Seq	Surf	Node	ALPHA	EMISS	TMASS	DISS	MID
1	1.00	1	0.700	0.770	0.	0.	97
2	2.00	2	0.790	0.85	.026	0.	439
3	3.00	3	0.160	0.700	.144	0.	130
4	4.00	4	0.790	0.85	.026	0.	439
5	5.00	5	0.160	0.700	.144	0.	130
6	6.00	6	0.790	0.85	.026	0.	439
7	7.00	7	0.160	0.700	.144	0.	130
8	8.00	8	0.790	0.85	.026	0.	439
9	9.00	9	0.160	0.700	.144	0.	130
10	10.00	10	0.790	0.85	.144	0.	439
11	11.00	11	0.790	0.85	.072	0.	439
12	12.00	12	0.790	0.85	.144	0.	439
13	13.00	13	0.790	0.85	.072	0.	439
14	14.00	14	0.790	0.85	.144	0.	439
15	15.00	15	0.790	0.85	.072	0.	439
16	16.00	16	0.790	0.85	.144	0.	439
17	17.00	17	0.790	0.85	.072	0.	439
18	18.00	18	0.790	0.85	.144	0.	439
19	19.00	19	0.160	0.700	.026	0.	130
20	20.00	20	0.790	0.85	.144	0.	439
21	21.00	21	0.160	0.700	.026	0.	130
22	22.00	22	0.790	0.85	.144	0.	439
23	23.00	23	0.160	0.700	.026	0.	130
24	24.00	24	0.790	0.85	.144	0.	439
25	25.00	25	0.160	0.700	.026	0.	130
26	26.00	26	0.790	0.85	.144	0.	439

PC-ITAS USER NODES

Node	Temp	TMass	Dissip	Description
1001	10.000	0.1440	0.0000	SA
1002	10.000	0.0266	0.0000	TRI
1003	10.000	0.1440	0.0000	SA
1004	10.000	0.0266	0.0000	TRI
1005	10.000	0.1440	0.0000	SA
1006	10.000	0.0266	0.0000	TRI
1007	10.000	0.1440	0.0000	SA
1008	10.000	0.0266	0.0000	TRI
1009	10.000	0.1440	0.0000	SA/TOP
1010	10.000	0.0900	0.0000	TOP SHELF/TOP BAY/

1011	10.000	0.0400	0.0000	TOP SHELF/TOP BAY/
1012	10.000	0.0900	0.0000	TOP SHELF/TOP BAY/
1013	10.000	0.0400	0.0000	TOP SHELF/TOP BAY/
1014	10.000	0.0900	0.0000	TOP SHELF/TOP BAY/
1015	10.000	0.0400	0.0000	TOP SHELF/TOP BAY/
1016	10.000	0.0900	0.0000	TOP SHELF/TOP BAY/
1017	10.000	0.0400	0.0000	TOP SHELF/TOP BAY/
1018	10.000	0.0900	0.0000	TOP SHELF/TOP BAY/
1019	10.000	0.0000	0.0000	RF COMM MOD (S)
1020	10.000	2.4000	0.0000	RF COMM MOD (b)
2001	10.000	0.1440	0.0000	SA
2002	10.000	0.0720	0.0000	SA
2003	10.000	0.1440	0.0000	SA
2004	10.000	0.0720	0.0000	SA
2005	10.000	0.1440	0.0000	SA
2006	10.000	0.0720	0.0000	SA
2007	10.000	0.1440	0.0000	SA
2008	10.000	0.0720	0.0000	SA
2009	10.000	0.0450	0.0000	BOT SHELF/MID BAY/
2010	10.000	0.0450	0.0000	BOT SHELF/MID BAY/
2011	10.000	0.0200	0.0000	BOT SHELF/MID BAY/
2012	10.000	0.0450	0.0000	BOT SHELF/MID BAY/
2013	10.000	0.0200	0.0000	BOT SHELF/MID BAY/
2014	10.000	0.0450	0.0000	BOT SHELF/MID BAY/
2015	10.000	0.0200	0.0000	BOT SHELF/MID BAY/
2016	10.000	0.0450	0.0000	BOT SHELF/MID BAY/
2017	10.000	0.0200	0.0000	BOT SHELF/MID BAY/
2018	10.000	0.0900	0.0000	TOP SHELF/MID BAY/
2019	10.000	0.0950	0.0000	TOP SHELF/MID BAY/
2020	10.000	0.0400	0.0000	TOP SHELF/MID BAY/
2021	10.000	0.0900	0.0000	TOP SHELF/MID BAY/
2022	10.000	0.0400	0.0000	TOP SHELF/MID BAY/
2023	10.000	0.0900	0.0000	TOP SHELF/MID BAY/
2024	10.000	0.0400	0.0000	TOP SHELF/MID BAY/
2025	10.000	0.0900	0.0000	TOP SHELF/MID BAY/
2026	10.000	0.0400	0.0000	TOP SHELF/MID BAY/
2027	10.000	0.0000	0.0000	EPS BOX (S)
2028	10.000	1.5600	0.0000	EPS BOX (B)
2029	10.000	0.0000	0.0000	DCS (S)
2030	10.000	1.9500	0.0000	DCS (B)
2031	10.000	0.0000	0.0000	BATTERY A (S)
2032	10.000	1.5600	0.0000	BATTERY A (B)
2033	10.000	0.0000	0.0000	BATTERY B (S)
2034	10.000	1.5600	0.0000	BATTERY B (S)
3001	10.000	0.0010	0.0000	BOT CLOSEOUT
3002	10.000	0.1440	0.0000	SA
3003	10.000	0.0266	0.0000	TRI
3004	10.000	0.1440	0.0000	SA
3005	10.000	0.0266	0.0000	TRI
3006	10.000	0.1440	0.0000	SA
3007	10.000	0.0266	0.0000	TRI
3008	10.000	0.1440	0.0000	SA
3009	10.000	0.0266	0.0000	TRI
3010	10.000	0.0450	0.0000	BOT SHELF/BOT BAY/
3011	10.000	0.0200	0.0000	BOT SHELF/BOT BAY/
3012	10.000	0.0450	0.0000	BOT SHELF/BOT BAY/
3013	10.000	0.0200	0.0000	BOT SHELF/BOT BAY/
3014	10.000	0.0450	0.0000	BOT SHELF/BOT BAY/

3015	10.000	0.0200	0.0000	BOT SHELF/BOT BAY/
3016	10.000	0.0450	0.0000	BOT SHELF/BOT BAY/
3017	10.000	0.0200	0.0000	BOT SHELF/BOT BAY/
3018	10.000	0.0450	0.0000	BOT SHELF/BOT BAY/

PC-ITAS Enclosure #1 Nodes: ENCLTOP.RAD

Seq	Node	Temp	TMass	Dissip	Comment
1	1001	10.0	0.144	0.000	SA
2	1002	10.0	0.027	0.000	TRI
3	1003	10.0	0.144	0.000	SA
4	1004	10.0	0.027	0.000	TRI
5	1005	10.0	0.144	0.000	SA
6	1006	10.0	0.027	0.000	TRI
7	1007	10.0	0.144	0.000	SA
8	1008	10.0	0.027	0.000	TRI
9	1009	10.0	0.144	0.000	SA/TOP
10	1010	10.0	0.090	0.000	TOP SHELF/TOP BAY/
11	1011	10.0	0.040	0.000	TOP SHELF/TOP BAY/
12	1012	10.0	0.090	0.000	TOP SHELF/TOP BAY/
13	1013	10.0	0.040	0.000	TOP SHELF/TOP BAY/
14	1014	10.0	0.090	0.000	TOP SHELF/TOP BAY/
15	1015	10.0	0.040	0.000	TOP SHELF/TOP BAY/
16	1016	10.0	0.090	0.000	TOP SHELF/TOP BAY/
17	1017	10.0	0.040	0.000	TOP SHELF/TOP BAY/
18	1018	10.0	0.090	0.000	TOP SHELF/TOP BAY/
19	1019	10.0	0.000	8.000	RF COMM MOD (S)
20	1020	10.0	2.400	0.000	RF COMM MOD (b)

NUMBER OF RADK FOR: ENCLTOP.RAD = 171

PC-ITAS Enclosure #2 Nodes: ENCLMID.RAD

Seq	Node	Temp	TMass	Dissip	Comment
1	2001	10.0	0.144	0.000	SA
2	2002	10.0	0.072	0.000	SA
3	2003	10.0	0.144	0.000	SA
4	2004	10.0	0.072	0.000	SA
5	2005	10.0	0.144	0.000	SA
6	2006	10.0	0.072	0.000	SA
7	2007	10.0	0.144	0.000	SA
8	2008	10.0	0.072	0.000	SA
9	2009	10.0	0.045	0.000	BOT SHELF/MID BAY/
10	2010	10.0	0.045	0.000	BOT SHELF/MID BAY/
11	2011	10.0	0.020	0.000	BOT SHELF/MID BAY/
12	2012	10.0	0.045	0.000	BOT SHELF/MID BAY/
13	2013	10.0	0.020	0.000	BOT SHELF/MID BAY/
14	2014	10.0	0.045	0.000	BOT SHELF/MID BAY/
15	2015	10.0	0.020	0.000	BOT SHELF/MID BAY/
16	2016	10.0	0.045	0.000	BOT SHELF/MID BAY/
17	2017	10.0	0.020	0.000	BOT SHELF/MID BAY/
18	2018	10.0	0.090	0.000	TOP SHELF/MID BAY/
19	2019	10.0	0.095	0.000	TOP SHELF/MID BAY/
20	2020	10.0	0.040	0.000	TOP SHELF/MID BAY/
21	2021	10.0	0.090	0.000	TOP SHELF/MID BAY/
22	2022	10.0	0.040	0.000	TOP SHELF/MID BAY/
23	2023	10.0	0.090	0.000	TOP SHELF/MID BAY/
24	2024	10.0	0.040	0.000	TOP SHELF/MID BAY/

25	2025	10.0	0.090	0.000	TOP SHELF/MID BAY/
26	2026	10.0	0.040	0.000	TOP SHELF/MID BAY/
27	2027	10.0	0.000	5.000	EPS BOX (S)
28	2028	10.0	1.560	0.000	EPS BOX (B)
29	2029	10.0	0.000	4.000	DCS (S)
30	2030	10.0	1.950	0.000	DCS (B)
31	2031	10.0	0.000	5.000	BATTERY A (S)
32	2032	10.0	1.560	0.000	BATTERY A (B)
33	2033	10.0	0.000	0.000	BATTERY B (S)
34	2034	10.0	1.560	0.000	BATTERY B (S)

NUMBER OF RADK FOR: ENCLMID.RAD = 435

PC-ITAS Enclosure #3 Nodes: ENCLBOT2.RAD

Seq	Node	Temp	TMass	Dissip	Comment
1	3001	10.0	0.001	0.000	
2	3002	10.0	0.144	0.000	
3	3003	10.0	0.027	0.000	
4	3004	10.0	0.144	0.000	
5	3005	10.0	0.027	0.000	
6	3006	10.0	0.144	0.000	
7	3007	10.0	0.027	0.000	
8	3008	10.0	0.144	0.000	
9	3009	10.0	0.027	0.000	
10	3010	10.0	0.045	0.000	BOT SHELF/BOT BAY/
11	3011	10.0	0.200	0.000	BOT SHELF/BOT BAY/
12	3012	10.0	0.045	0.000	BOT SHELF/BOT BAY/
13	3013	10.0	0.200	0.000	BOT SHELF/BOT BAY/
14	3014	10.0	0.045	0.000	BOT SHELF/BOT BAY/
15	3015	10.0	0.200	0.000	BOT SHELF/BOT BAY/
16	3016	10.0	0.045	0.000	BOT SHELF/BOT BAY/
17	3017	10.0	0.200	0.000	BOT SHELF/BOT BAY/
18	3018	10.0	0.045	0.000	BOT SHELF/BOT BAY/
19	3020	10.0	0.160	0.000	CYL SURFACE (INTER

NUMBER OF RADK FOR: ENCLBOT2.RAD= 171

 PC-ITAS USER CONDUCTANCES

Seq	Fact	From	To	Cond	L/R	Description
1	1	1	3001	1	L	MYLAR CLOSEOUT
2	1	2	3002	7500	L	SOLAR ARRAY OUTSIDE TO INSIDE
3	1	3	3003	2700	L	SA
4	1	4	3004	7500	L	SA
5	1	5	3005	2700	L	SA
6	1	6	3006	7500	L	SA
7	1	7	3007	2700	L	SA
8	1	8	3008	7500	L	SA
9	1	9	3009	2700	L	SA
10	1	10	2001	7500	L	SA
11	1	11	2002	7500	L	SA
12	1	12	2003	7500	L	SA
13	1	13	2004	7500	L	SA
14	1	14	2005	7500	L	SA
15	1	15	2006	7500	L	SA

16	1	16	2007	7500	L SA
17	1	17	2008	7500	L SA
18	1	18	1001	7500	L SA
19	1	19	1002	2700	L SA
20	1	20	1003	7500	L SA
21	1	21	1004	2700	L SA
22	1	22	1005	7500	L SA
23	1	23	1006	2700	L SA
24	1	24	1007	7500	L SA
25	1	25	1008	2700	L SA
26	1	26	1009	7500	L SA
27	1	1010	1012	1.2	L TOP DECK CENTER TO SIDE
28	1	1010	1014	1.2	L TP DE
29	1	1010	1016	1.2	L TP DE
30	1	1010	1018	1.2	L TP DE
31	1	1012	1013	.8	L TOP DECK PERIMETER
32	1	1013	1014	.8	L TP DE
33	1	1014	1015	.8	L TP DE
34	1	1015	1016	.8	L TP DE
35	1	1016	1017	.8	L TP DE
36	1	1017	1018	.8	L TP DE
37	1	1018	1011	.8	L TP DE
38	1	1011	1012	.8	L TP DE
39	1	1019	1020	100	L RF BOX SIDE TO BASE
40	1	1020	1010	8.5	L RF BOX BASE TO DECK
41	1	1020	1011	2.5	L RF BX BS TO DK
42	1	1020	1015	2.5	L RF BX BS TO DK
43	1	1009	1001	1.2	L TOP SA TO SIDE SA
44	1	1009	1003	1.2	L SA
45	1	1009	1005	1.2	L SA
46	1	1009	1007	1.2	L SA
47	1	1001	1002	.31	L PERIMETER SOLAR ARRAYS
48	1	1002	1003	.31	L SA
49	1	1003	1004	.31	L SA
50	1	1004	1005	.31	L SA
51	1	1005	1006	.31	L SA
52	1	1006	1007	.31	L SA
53	1	1007	1008	.31	L SA
54	1	1008	1001	.31	L SA
55	1	2001	2002	.31	L SA AROUND PERIMETER OF MID BAY
56	1	2002	2003	.31	L SA
57	1	2003	2004	.31	L SA
58	1	2004	2005	.31	L SA
59	1	2005	2006	.31	L SA
60	1	2006	2007	.31	L SA
61	1	2007	2008	.31	L SA
62	1	2008	2001	.31	L SA
63	1	2010	2011	.4	L BOT DECK TOP SURFACE PERIM
64	1	2011	2012	.4	L BOT DK
65	1	2012	2013	.4	L BOT DK
66	1	2013	2014	.4	L BOT DK
67	1	2014	2015	.4	L BOT DK
68	1	2015	2016	.4	L BOT DK
69	1	2016	2017	.4	L BOT DK
70	1	2017	2018	.4	L BOT DK
71	1	2009	2011	.6	L BOTTOM DECK CENTER TO SIDES
72	1	2009	2013	.6	L BOT DK
73	1	2009	2015	.6	L BOT DK

74	1	2009	2017	.6	L BOT DK
75	1	2019	2020	.8	L TOP DECK BOTTOM SURACE PERIM
76	1	2020	2021	.8	L TP DK
77	1	2021	2022	.8	L TP DK
78	1	2022	2023	.8	L TP DK
79	1	2023	2024	.8	L TP DK
80	1	2024	2025	.8	L TP DK
81	1	2025	2026	.8	L TP DK
82	1	2026	2027	.8	L TP DK
83	1	2018	2020	1.2	L TOP DECK CENTER TO SIDES
84	1	2018	2022	1.2	L TP DK
85	1	2018	2024	1.2	L TP DK
86	1	2018	2026	1.2	L TP DK
87	1	2027	2028	25	L EPS BOX SIDE TO BASE
88	1	2029	2030	25	L DCS BOX SIDE TO BASE
89	1	2031	2032	25	L BATTERY SIDE TO BASE
90	1	2033	2034	25	L BATTERY SIDE TO BASE
91	1	3001	3002	.001	L MYLAR CLOSE OUT TO SIDE SA
92	1	3001	3004	.001	L MYL
93	1	3001	3006	.001	L MYL
94	1	3001	3008	.001	L MYL
95	1	3002	3003	.31	L SA AROUND PERIMETER
96	1	3003	3004	.31	L SA
97	1	3004	3005	.31	L SA
98	1	3005	3006	.31	L SA
99	1	3006	3007	.31	L SA
100	1	3007	3008	.31	L SA
101	1	3008	3009	.31	L SA
102	1	3009	3002	.31	L SA
103	1	3011	3012	.4	L BOTTM DECK PERIMETER
104	1	3012	3013	.4	L BT DE
105	1	3013	3014	.4	L BT DE
106	1	3014	3015	.4	L BT DE
107	1	3015	3016	.4	L BT DE
108	1	3016	3017	.4	L BT DE
109	1	3017	3018	.4	L BT DE
110	1	3018	3011	.4	L BT DE
111	1	3010	3012	.6	L BOTTOM DECK CENTER TO DSIDE
112	1	3010	3014	.6	L BT DE
113	1	3010	3016	.6	L BT DE
114	1	3010	3018	.6	L BT DE
115	1	2028	2018	14.9	L EPS BOX BASE TO DECK
116	1	2030	2018	1	L DCS BOX TO BASE
117	1	2030	2020	1	L DCS BX TO BS
118	1	2030	2022	1	L DCS BX TO BS
119	1	2030	2024	1	L DCS BX TO BS
120	1	2030	2026	1	L DCS BX TO BS
121	1	2034	2010	7	L BATTERY A TO DECK
122	1	2034	2011	2.1	L BAT
123	1	2034	2017	2.1	L BAT
124	1	2032	2014	7	L BATTERY B TO DECK
125	1	2032	2013	2.1	L BAT
126	1	2032	2015	2.1	L BAT
127	1	3020	3010	1.26	L TUBE TO DECK
128	1	3020	3001	.001	L TUBE TO MYLAR
129	1	3002	3018	1.26	L BOT SA TO dECK
130	1	3003	3011	1.26	L SA/DE
131	1	3004	3012	1.26	L SA/DE

132	1	3005	3013	1.26	L SA/DE
133	1	3006	3014	1.26	L SA/DE
134	1	3007	3015	1.26	L SA/DE
135	1	3008	3016	1.26	L SA/DE
136	1	3009	3017	1.26	L SA/DE
137	1	2001	2017	.31	L MID SA TO BOT DE
138	1	2002	2010	1.26	L SA/DE
139	1	2003	2011	.31	L SA/DE
140	1	2004	2012	1.26	L SA/DE
141	1	2005	2013	.31	L SA/DE
142	1	2006	2014	1.26	L SA/DE
143	1	2007	2015	.31	L SA/DE
144	1	2008	2016	1.26	L SA/DE
145	1	2001	2026	.31	L MID SA TO UPPER DECK
146	1	2002	2019	1.26	L SA/DE
147	1	2003	2020	.31	L SA/DE
148	1	2004	2021	1.26	L SA/DE
149	1	2005	2022	.31	L SA/DE
150	1	2006	2023	1.26	L SA/DE
151	1	2007	2024	.31	L SA/DE
152	1	2008	2025	1.26	L SA/DE
153	1	1001	1018	1.26	L TOP SA TO UPPER DECK
154	1	1002	1011	1.26	L SA/DE
155	1	1003	1012	1.26	L SA/DE
156	1	1004	1013	1.26	L SA/DE
157	1	1005	1014	1.26	L SA/DE
158	1	1006	1015	1.26	L SA/DE
159	1	1007	1016	1.26	L SA/DE
160	1	1008	1017	1.26	L SA/DE
161	1	1010	2018	1820	L TOP DECK THROUGH CONDUCTANCE
162	1	1011	2019	360	L DE
163	1	1012	2020	1146	L DE
164	1	1013	2021	360	L DE
165	1	1014	2022	1146	L DE
166	1	1015	2023	360	L DE
167	1	1016	2024	1146	L DE
168	1	1017	2025	360	L DE
169	1	1018	2026	1146	L DE
170	1	3010	2009	910	L BOTTOM DECK THOUGH CONDUCTANCE
171	1	3011	2010	180	L DE
172	1	3012	2011	573	L DE
173	1	3013	2012	180	L DE
174	1	3014	2013	573	L DE
175	1	3015	2014	180	L DE
176	1	3016	2015	573	L DE
177	1	3017	2016	180	L DE
178	1	3018	2017	573	L DE

PC-ITAS USER DEFINED CONSTANTS (UDC)

END OF PC-ITAS NODE & CONDUCTANCE REPORT

APPENDIX D

This table provides the steady state temperatures for every node in the PANSAT thermal model, for both the hot case and cold cases described in the text.

Node	Hot Case (Deg F)	Cold Case (Deg F)		Node	Hot Case (Deg F)	Cold Case (Deg F)
1	33.84	16.83		1013	48.34	10.63
2	36.79	15.78		1014	44.19	12.00
3	44.42	9.55		1015	41.25	11.34
4	56.82	11.30		1016	38.37	11.30
5	46.29	8.37		1017	34.39	11.12
6	39.90	11.80		1018	41.90	13.57
7	33.87	8.31		1019	47.55	13.86
8	24.94	8.53		1020	47.28	13.71
9	26.53	7.72		2001	36.25	18.41
10	36.25	18.41		2002	57.40	13.35
11	57.42	13.35		2003	76.64	2.97
12	76.66	2.97		2004	55.49	7.75
13	55.49	7.75		2005	41.05	8.92
14	41.05	8.92		2006	34.18	7.21
15	34.18	7.21		2007	19.15	-2.25
16	19.15	-2.25		2008	24.17	9.63
17	24.17	9.63		2009	42.71	11.25
18	38.19	16.52		2010	48.16	11.64
19	43.88	10.78		2011	49.35	10.94
20	52.11	13.23		2012	48.87	9.18
21	45.25	10.02		2013	42.04	10.81
22	40.75	13.32		2014	38.86	9.99
23	36.46	10.08		2015	36.59	9.84
24	30.88	11.37		2016	30.85	9.72
25	29.93	9.21		2017	42.12	12.51
26	39.65	15.04		2018	45.81	13.19
1001	38.19	16.52		2019	48.33	12.78
1002	43.90	10.78		2020	49.42	12.06
1003	52.11	13.23		2021	48.36	10.63
1004	45.25	10.02		2022	44.20	12.00
1005	40.75	13.32		2023	41.23	11.32
1006	36.46	10.08		2024	38.37	11.28
1007	30.88	11.37		2025	34.38	11.12
1008	29.93	9.21		2026	41.90	13.57
1009	39.65	15.04		2027	47.08	13.80
1010	45.81	13.19		2028	46.60	13.55
1011	48.29	12.78		2029	44.89	11.75
1012	49.42	12.06		2030	44.51	11.64

Steady State Temperatures

Node	Hot Case (Deg F)	Cold Case (Deg F)		Node	Hot Case (Deg F)	Cold Case (Deg F)
2031	41.16	10.94		3009	26.55	7.72
2032	40.50	10.69		3010	42.71	11.25
2033	47.43	11.73		3011	48.13	11.64
2034	47.39	11.73		3012	49.37	10.94
3001	33.84	16.83		3013	48.85	9.18
3002	36.79	15.78		3014	42.04	10.81
3003	44.42	9.55		3015	38.82	9.97
3004	56.82	11.30		3016	36.57	9.84
3005	46.29	8.37		3017	30.87	9.72
3006	39.90	11.80		3018	42.10	12.51
3007	33.87	8.31		3020	42.31	11.57
3008	24.94	8.53		9999	-459.69	-459.69

Steady State Temperatures

This table provides the temperature extremes seen by every node in the PANSAT thermal model, for both the hot case and cold cases described in the text, i.e. the hottest hot case temperatures and the coldest cold case temperatures

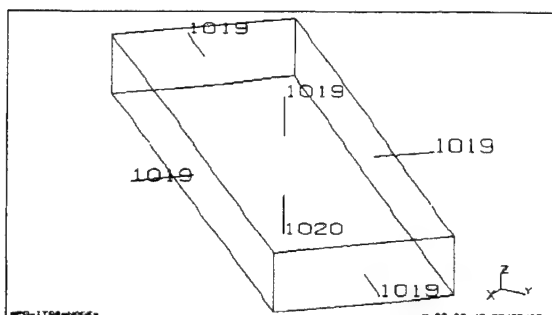
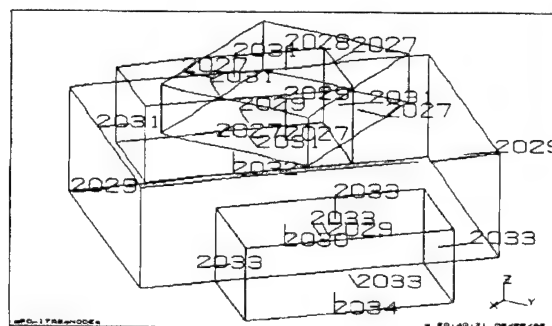
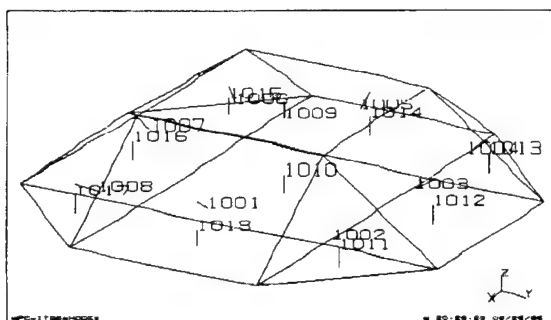
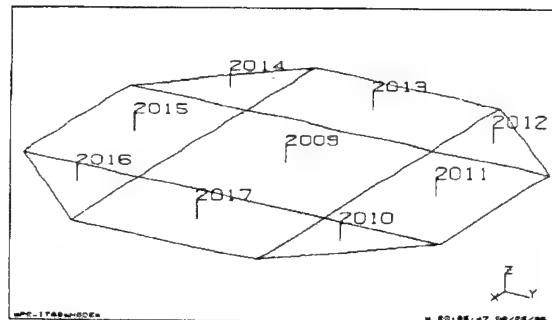
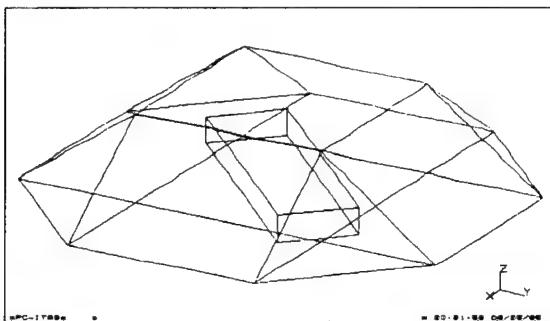
Node	Hot Case (Deg F)	Cold Case (Deg F)		Node	Hot Case (Deg F)	Cold Case (Deg F)
1.00	30.97	-30.63		21.00	20.35	-17.79
2.00	16.49	-23.17		22.00	21.66	-18.45
3.00	13.64	-19.14		23.00	8.15	-17.25
4.00	31.46	-21.09		24.00	6.86	-20.96
5.00	13.02	-17.59		25.00	3.91	-20.63
6.00	12.89	-18.20		26.00	21.39	-21.76
7.00	1.93	-16.77		1001.00	15.53	-21.89
8.00	-2.09	-21.26		1002.00	15.19	-18.65
9.00	-0.47	-21.01		1003.00	31.43	-20.59
10.00	17.98	-24.83		1004.00	20.35	-17.79
11.00	26.21	-19.24		1005.00	21.67	-18.45
12.00	37.79	-21.01		1006.00	8.15	-17.25
13.00	26.15	-16.15		1007.00	6.86	-20.96
14.00	11.07	-15.28		1008.00	3.91	-20.62
15.00	2.52	-15.42		1009.00	21.38	-21.76
16.00	-6.25	-22.14		1010.00	11.22	-13.47
17.00	-1.94	-21.90		1011.00	13.87	-14.84
18.00	15.53	-21.89		1012.00	18.12	-15.53
19.00	15.18	-18.65		1013.00	18.79	-15.76
20.00	31.44	-20.59		1014.00	13.84	-15.16

Extreme Temperatures

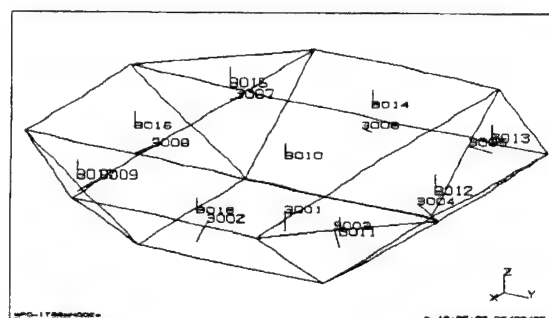
Node	Hot Case (Deg F)	Cold Case (Deg F)		Node	Hot Case (Deg F)	Cold Case (Deg F)
1015.00	9.10	-14.82		2025.00	5.31	-17.90
1016.00	7.81	-16.14		2026.00	10.06	-15.99
1017.00	5.32	-17.90		2027.00	11.47	-12.94
1018.00	10.07	-16.00		2028.00	11.24	-13.10
1019.00	11.50	-12.70		2029.00	8.68	-13.46
1020.00	11.36	-12.76		2030.00	8.39	-13.47
2001.00	17.98	-24.83		2031.00	5.90	-13.63
2002.00	26.21	-19.23		2032.00	5.53	-13.77
2003.00	37.78	-21.01		2033.00	12.15	-15.22
2004.00	26.15	-16.15		2034.00	12.10	-15.21
2005.00	11.08	-15.28		3001.00	30.97	-30.63
2006.00	2.52	-15.42		3002.00	16.49	-23.17
2007.00	-6.25	-22.14		3003.00	13.64	-19.14
2008.00	-1.93	-21.89		3004.00	31.46	-21.08
2009.00	8.11	-15.51		3005.00	13.03	-17.59
2010.00	13.49	-15.95		3006.00	12.89	-18.20
2011.00	13.60	-16.20		3007.00	1.93	-16.77
2012.00	13.34	-15.92		3008.00	-2.09	-21.26
2013.00	6.68	-15.01		3009.00	-0.47	-21.01
2014.00	4.56	-14.31		3010.00	8.11	-15.51
2015.00	3.70	-16.10		3011.00	13.46	-15.97
2016.00	1.29	-18.91		3012.00	13.62	-16.21
2017.00	9.23	-16.73		3013.00	13.27	-15.92
2018.00	11.22	-13.47		3014.00	6.69	-15.02
2019.00	13.90	-14.85		3015.00	4.54	-14.32
2020.00	18.11	-15.52		3016.00	3.69	-16.11
2021.00	18.79	-15.76		3017.00	1.29	-18.90
2022.00	13.84	-15.16		3018.00	9.24	-16.74
2023.00	9.08	-14.83		3020.00	8.25	-15.48
2024.00	7.80	-16.13		9999.00	-273.16	-273.16

Extreme Temperatures

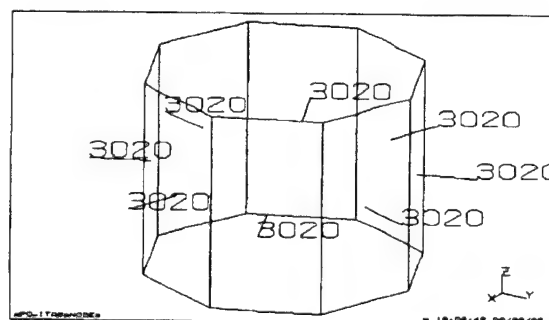
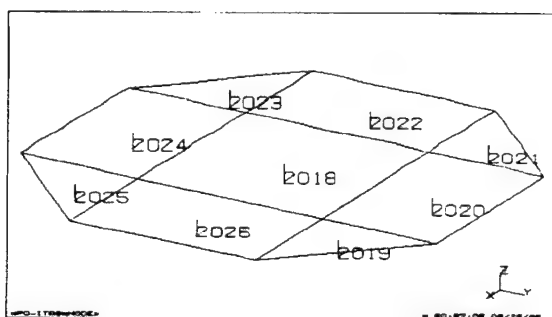
Upper Enclosure Nodes



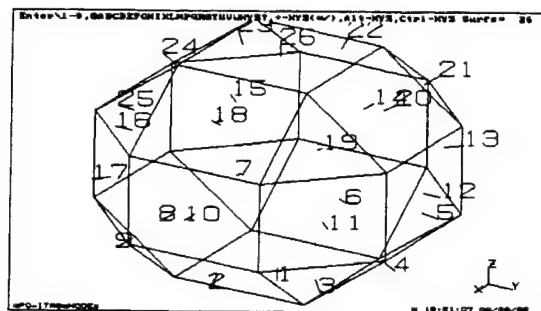
Bottom Enclosure Nodes



Middle Enclosure Nodes



Outer Shell Model



REFERENCES

1. Agrawal, B.B., *Design Of Geosynchronous Spacecraft*, Prentice Hall, Englewood Cliffs, New Jersey, 1986, pp. 265-268.
2. Agrawal, B.B., p. 267
3. Holman, J.P., *Heat Transfer*, McGraw-Hill Book Company, New York, 1981, pp. 305-335.
4. Noravian, H., *Integrated Thermal Analysis System - Users Manual*, Analytix Corporation, Timonium, Maryland 1994, pp. 4.1 - 4.12.
5. Noravian, H., pp 8.1 - 8.6
6. Gilmore, David G., *Satellite Thermal Control Handbook*, The Aerospace Corporation Press, El Segundo, CA, 1994, pp. 4.19 - 4.30
7. Gilmore, David G., pp. 4.38 - 4.59
8. Gilmore, David G., pp. 4.38 - 4.59
9. Agrawal, B.B., p. 286
10. Anderson, Jeff and Smith, Robert E., *Natural Orbital Environmental Guidelines for Use in Aerospace Vehicle Development*, NASA Technical Memorandum 4527, June 1994, pp. 9.1 - 9.17
11. Wertz, James R. and Larson, Wiley J., *Space Mission Analysis And Design*, Kluwer Academic Publishers, Boston, Massachusetts, 1991, pp. 370-386
12. Department Of Defense, MIL-STD-1540-B, *Test Requirements For Space Vehicles*, Government Printing Office, Washington, DC, 1982
13. Department Of Defense, DOD-HDBK-343 (USAF), *Design, Construction, And Testing Requirements For One Of A Kind Spacecraft*, Government Printing Office, Washington, DC, 1986

INITIAL DISTRIBUTION LIST

- | | | |
|----|---|---|
| 1. | Defense Technical Information Center
Cameron Station
Alexandria, VA 22304-6145 | 2 |
| 2. | Library, Code 52
Naval Postgraduate School
Monterey, CA 93943-5101 | 2 |
| 3. | Chairman, Code SP
Department of Aeronautics and Astronautics
Naval Postgraduate School
Monterey, CA 93943 | 1 |
| 4. | Professor Allan Kraus, Code EC/KS
Department of Electrical and Computer Engineering
Naval Postgraduate School
Monterey, CA 93943 | 1 |
| 5. | Mr. Nelson Hyman
Naval Research Laboratory, Code 8220
4555 Overlook Ave., S.W.
Washington, DC 20375-5320 | 1 |
| 6. | Mr. Nick Davinic
Naval Research Laboratory, Code 8222
4555 Overlook Ave., S.W.
Washington, DC 20375-5320 | 2 |